HHS Public Access

Author manuscript

Mol Microbiol. Author manuscript; available in PMC 2017 August 01.

Published in final edited form as:

Mol Microbiol. 2016 August ; 101(3): 495–514. doi:10.1111/mmi.13404.

A Spectrum of CodY Activities Drives Metabolic Reorganization and Virulence Gene Expression in *Staphylococcus aureus*

Nicholas R. Waters[a], **David J. Samuels**[a], **Ranjan K. Behera**[a], **Jonathan Livny**[b], **Kyu Y. Rhee**[c], **Marat R. Sadykov**[d], and **Shaun R. Brinsmade**[a,#]

[a]Department of Biology, Georgetown University, Washington, District of Columbia, USA

[b]Broad Institute of MIT and Harvard, Cambridge, Massachusetts, USA

[c]Division of Infectious Diseases, Department of Medicine, Weill Cornell Medical College, New York, New York, USA

[d]Department of Pathology and Microbiology, University of Nebraska Medical Center, Omaha, Nebraska 68198

Abstract

The global regulator CodY controls the expression of dozens of metabolism and virulence genes in the opportunistic pathogen *Staphylococcus aureus* in response to the availability of isoleucine, leucine and valine (ILV), and GTP. Using RNA-Seq transcriptional profiling and partial activity variants, we reveal that *S. aureus* CodY activity grades metabolic and virulence gene expression as a function of ILV availability, mediating metabolic reorganization and controlling virulence factor production in vitro. Strains lacking CodY regulatory activity produce a PIA-dependent biofilm, but development is restricted under conditions that confer partial CodY activity. CodY regulates the expression of thermonuclease (*nuc*) via the Sae two-component system, revealing cascading virulence regulation and factor production as CodY activity is reduced. Proteins that mediate the host-pathogen interaction and subvert the immune response are shut off at intermediate levels of CodY activity, while genes coding for enzymes and proteins that extract nutrients from tissue, that kill host cells, and that synthesize amino acids are among the last genes to be de-repressed. We conclude that *S. aureus* uses CodY to limit host damage to only the most severe starvation conditions, providing insight into one potential mechanism by which *S. aureus* transitions from a commensal bacterium to an invasive pathogen.

Graphical abstract

[#]Address correspondence to Shaun Brinsmade, shaun.brinsmade@georgetown.edu Tel. 202-687-6549 Fax. 202-687-5662.

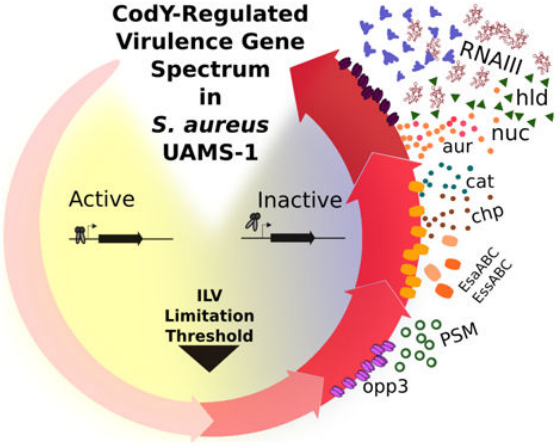

Keywords

CodY; *Staphylococcus aureus*; virulence; regulation; branched-chain amino acids

Introduction

Staphylococcus aureus is a ubiquitous, Gram-positive commensal bacterium that asymptomatically colonizes the anterior nare epithelium of 20% of the human population stably and 30% of the population intermittently (Lowy, 1998, Casewell & Hill, 1986, Noble *et al.*, 1967). However, under permissive conditions, *S. aureus* converts to an opportunistic pathogen and is the leading cause of skin and soft tissue infections, pneumonia, endocarditis, peritonitis, osteomyelitis, bacteremia, and sepsis (Salgado-Pabón *et al.*, 2013, Lowy, 1998, Kumar *et al.*, 2015, Gillaspy *et al.*, 1995a, Bubeck Wardenburg *et al.*, 2007). In addition to healthcare-associated infections, community-acquired infections are increasing in frequency and pose a major health threat to otherwise healthy individuals (Herold *et al.*, 1998, Naimi *et al.*, 2003). The augmented capacity of community-acquired strains to cause disease has been attributed to the acquisition of genes that encode Panton-Valentine Leukocidin (PVL) and genes that provide for wider metabolic versatility during survival on host skin (Joshi *et al.*, 2011, Vandenesch *et al.*, 2003). Indeed, *S. aureus* is a successful pathogen largely due to its metabolic versatility and its ability to subvert the immune response.

S. aureus virulence genes encode a vast arsenal of surface-associated and secreted factors that are deployed in stages, allowing the bacterium to survive and replicate in the host (Cheng *et al.*, 2009). These genes can be separated into two major categories: one containing genes that mediate colonization; the other containing genes that mediate tissue damage and cellular toxicity (Novick, 2003). Regulation of virulence gene expression is complex and is tightly controlled by a plethora of Two-Component Systems (TCSs), global regulators and small RNAs that sense a variety of signals including growth phase and population density. Notable regulators include SaeRS, repressor of toxins Rot, the alternative sigma factor B (SigB), the Sar family of proteins and RNAIII (Cheung *et al.*, 2008, Giraudo *et al.*, 1999, McNamara *et al.*, 2000, Recsei *et al.*, 1986, Wu *et al.*, 1996). Because survival and growth in

the host requires the scavenging of essential nutrients (Weinberg, 1975), nutrient availability and virulence are inextricably linked.

The global transcriptional regulator CodY directly or indirectly controls the expression of over 200 genes in *S. aureus* (Majerczyk *et al.*, 2010, Pohl *et al.*, 2009). CodY acts mainly as a repressor of metabolic genes and virulence genes, though CodY stimulates a small number of genes as well. CodY is activated as a DNA-binding protein by two known classes of effectors: the branched-chain amino acids isoleucine, leucine and valine (ILV) and GTP, effectively linking the nutritional status of the cell with the production of virulence factors (Majerczyk *et al.*, 2010). Although the site of GTP binding has remained elusive, isoleucine and valine have been shown crystallographically to bind to the N-terminal GAF domain of the *Bacillus subtilis* CodY protein (Levdikov *et al.*, 2006). The interaction with ILV triggers a substantial conformational change that facilitates binding to a site-specific DNA sequence first recognized in *Lactococcus lactis* and revised specifically for *S. aureus* that is essential for full regulation of its targets (den Hengst *et al.*, 2005, Levdikov *et al.*, 2009, Majerczyk *et al.*, 2010). CodY regulates many of the virulence genes indirectly by regulating the *agr* locus and the levels of RNAIII by an as yet unknown mechanism. Recently, CodY was shown to be capable of overriding the quorum sensing control of *agr*-mediated gene expression, emphasizing that nutrient availability is a major factor in adjusting virulence gene expression (Roux *et al.*, 2014).

Changes in medium composition, growth rate, and physiological state present significant challenges when measuring expression of gene targets in vitro under nutrient depletion. For one, factors other than the regulator of interest can alter gene expression. We previously reported that genes within the CodY regulon in *B. subtilis* are controlled in a hierarchical manner using a method that exploits the known structure of CodY (Brinsmade *et al.*, 2014). Herein, we report that in *S. aureus,* strains producing CodY proteins with single-amino acid substitutions in the ILV binding pocket retain varying amounts of residual regulatory activity and mimic situations of decreasing ILV availability where the fraction of active CodY is sequentially reduced; such graded expression is likely reflective of the true mechanism of regulation during the host-pathogen interaction. Using RNA-Seq, we found clear transcriptional trends to prioritize amino acid metabolism pathways upon onset of nutrient limitation. Targeted metabolite profiling supported the transcriptional response, revealing alterations in steady-state abundance of several amino acids and their precursors. As the simulated nutrient limitation became more severe, we observed de-repression of genes whose products mediate biofilm development, destruction of host tissue, immune response evasion and dissemination. In doing so, we present, to our knowledge, the first such analysis for a global regulator in a pathogen, providing a foundation for determining the strategy by which *S. aureus* integrates metabolism and virulence functions relevant to infection.

Results

CodY target gene expression level changes as nutrients are depleted in vitro

The DNA-binding activity of *S. aureus* CodY is modulated by ILV and GTP (Majerczyk *et al.*, 2010). Thus, CodY-dependent genes should exhibit changes in expression level if these nutrients are depleted. To test this hypothesis, we isolated RNA from the USA200

methicillin-sensitive nosocomial osteomyelitis isolate UAMS-1 (Gillaspy *et al.*, 1995a) during exponential growth in chemically defined medium (CDM) (Hussain *et al.*, 1991) with decreasing ILV concentrations and performed quantitative, real-time RT-PCR (qRT-PCR) analysis on two gene targets that are repressed by CodY: *ilvD* (coding for dihydroxy acid dehydratase) and *hld* (coding for delta toxin) (Fink, 1993, Janzon *et al.*, 1989, Majerczyk *et al.*, 2010, Pohl *et al.*, 2009). We used UAMS-1 for the bulk of our studies because the CodY effect is well-characterized in this genetic background and a reference genome was recently published (Sassi *et al.*, 2015). In CDM medium containing 1,500 μM ILV (a concentration that maximizes potential CodY activity), *ilvD* and *hld* were de-repressed 147- and 59-fold in the *codY* mutant relative to the UAMS-1 wild-type strain, respectively (**Table 1**). Because the expression levels of *ilvD* and *hld* differ greatly in magnitude, we assigned an expression value of 0% for each gene in UAMS-1 (WT; CodY activity is maximal) and 100% for each gene in the *codY* null mutant (no CodY activity) during growth with 1,500 μM ILV. We then calculated expression relative to these levels for each gene during growth in CDM with concentrations of ILV spanning three orders of magnitude. *ilvD* expression in UAMS-1 increased to a level similar to that observed in the *codY* null mutant when ILV was reduced to 15 μM (**Table 1**). In contrast, *hld* expression increased only moderately, achieving an expression level at 1.5 μM ILV that is ~10% of that measured in the *codY* null mutant (**Table 1**).

During exponential growth, intracellular ILV and GTP pools are expected to be relatively high, maximizing CodY activity. However, entrance into post-exponential and stationary phases is expected to coincide with nutrient depletion, a condition monitored by CodY. To determine the extent to which CodY activity is retained under these conditions, we constructed a *nuc-gfp* transcriptional fusion (*nuc* is repressed by CodY (Majerczyk *et al.*, 2010)) and followed the production of GFP throughout the growth cycle. During exponential growth in tryptic soy broth (TSB; a rich, complex medium), *nuc-gfp* remained repressed in UAMS-1 and cells exhibited relatively low fluorescence (**Fig 1,** 0-2 h, grey circles). As the culture exited exponential phase, we measured an increase in fluorescence; the pattern of fluorescence was essentially identical to that observed in the *codY* null mutant, though the magnitude was higher. In fact, fluorescence increased nearly continuously from 0-3.5 h as expected given CodY's role in overriding the population density signal (Roux *et al.*, 2014); at 3.5 h *nuc-gfp* expression was ~12-fold higher relative to that measured in UAMS-1 at the same time point. Taken together, our results show that CodY target gene expression can be modulated by severe ILV limitation in defined medium, but mild nutrient depletion during post-exponential growth in TSB does not lead to significant loss of presumably potent CodY-mediated repression of *nuc-gfp*. Moreover, some gene targets appear to be more sensitive to perturbations in CodY activity than others.

Staphylococcus aureus uses CodY to regulate metabolism and virulence genes sequentially

Although one can determine the threshold level of CodY activity required to turn on and off various genes using the methods described above, these experimental designs remain uncontrolled for physiological state, changes in growth rate, and factors that alter expression when the medium composition is changed. The analysis of *Bacillus subtilis* strains

producing variant CodY proteins with varying amounts of residual DNA-binding activity revealed graded gene expression (Brinsmade *et al.*, 2014) and avoids such experimental design problems. Using the crystal structure of *B. subtilis* CodY as a guide (80% overall similarity to *S. aureus* CodY; 76% similar for residues 1-155 containing the GAF domain in which the ILV-binding pocket is located), we targeted a conserved arginine residue at position 61, substituting a variety of amino acids that alter the biochemical properties of this key ligand-interacting residue (Levdikov *et al.*, 2006). Alleles coding for these proteins were constructed using allelic exchange at the native *codY* locus in UAMS-1 to preserve the native regulation and copy number. Using qRT-PCR, we empirically and indirectly screened the activity of the resulting variant proteins by measuring transcript abundance for select CodY-regulated genes during steady-state exponential growth in TSB. As in *B. subtilis*, Arg61 proved to be a critical residue: $CodY^{R61K}$, $CodY^{R61H}$ and $CodY^{R61E}$ proteins retain varying amounts of residual activity as judged by the loss of regulation of known repressed and stimulated gene targets. Relatively low regulatory activity was measured for an additional variant substituting aspartate for glycine at position 129 ($CodY^{G129D}$) near the ILV binding pocket (**Fig. S1**). Cellular abundance and mobility of our CodY variants remained virtually unchanged compared to the wild-type UAMS-1 protein as judged by immunoblot analysis, suggesting that the CodY variants are stable and changes in gene expression are the result of changes in CodY specific activity (**Fig S2**). Collectively, our strains producing either wild-type CodY or a mutant version of CodY reflect the fraction of active CodY at varying levels of nutrient depletion; the *codY* null mutant behaves as though ILV are depleted.

To systematically profile CodY regulation of gene expression, we generated RNA-Seq data from UAMS-1 and the CodY mutant strains described above during exponential growth in TSB (see *Experimental Procedures*). Under these conditions, ILV and GTP pools are highest, CodY activity is maximized and cells are at physiological steady state, allowing for a robust, genome-wide measurement of the response to decreasing nutrients likely experienced in vivo without confounding variables associated with medium composition or growth rate changes.

We first compared RNA-Seq data from UAMS-1 and its *codY* null mutant to generate a list of genes under CodY control and to determine the extent to which each gene is maximally regulated. We identified 353 genes negatively regulated (i.e., repressed) by CodY and 29 genes positively regulated (i.e., stimulated) by CodY (fold change > 2, adjusted p-value <0.01). The RNA-Seq data compare favorably to our independent validation by qRT-PCR (**Table 2**). There was significant overlap between the list of CodY targets revealed by our analysis and those identified previously (Majerczyk *et al.*, 2010, Pohl *et al.*, 2009). Genes overexpressed in the null mutant (i.e., repressed by CodY) include direct and indirect targets of CodY and were the most strongly regulated; the *ilv-leu* operon that codes for enzymes and proteins for ILV synthesis showed the highest derepression (~200- to ~800-fold) (**Dataset S1**). Genes under-expressed in UAMS-1 (i.e., under positive CodY control) were at most ~11-fold regulated (**Dataset S2**). Comparison with previous microarray experiments yielded some exceptions. For example, we failed to detect significant upregulation of *rot*, autolysin SAR2040 or the putative transcriptional regulator SA2585 (Majerczyk *et al.*, 2010,

Pohl *et al.*, 2009). Strain differences, cultivation conditions, the high false discovery rate of microarrays and the signal-to-noise ratio in both RNA-Seq and microarray approaches when trying to observe relatively small differences in transcript abundance may account for these discrepancies.

Using a fixed concentration of active CodY, Majerczyk *et al.* identified differential enrichment of chromosomal regions containing putative CodY sequence motifs with varying degrees of degeneracy relative to a consensus sequence, suggesting that the *S. aureus* CodY protein transiently occupies its many sites based the active fraction of CodY to generate a graded response to nutrient availability. If true, we reasoned that we should be able to identify groups of genes whose expression patterns were similar. To that end, we applied a *k*-means cluster-based approach (Tavazoie *et al.*, 1999). We first assigned an expression value of 100% for repressed genes in the *codY* null mutant; positively regulated genes were set to 100% in UAMS-1. We then calculated expression relative to these levels for each gene across the set of strains producing CodY proteins with partial regulatory activity. To identify the optimum number of clusters, we examined the distribution of genes in as few as two and as many as 10 clusters each for repressed and stimulated genes. We chose six clusters (four and two, respectively) because the responses to changes in CodY activity were clearly differentiated. As in *B. subtilis,* we observed variable sensitivity of genes to changes in CodY activity (**Dataset S3, Fig. S3**). For example, Clusters 5 and 6 contained the positively regulated genes; on average, genes most sensitive to changes in CodY activity (cluster 5) showed <20% expression in the $CodY^{R61K}$-producing strain. Cluster 6 contained genes whose average expression level dropped below 20% in the R61E mutant. Negatively regulated genes fell into four clusters. Those genes most sensitive to changes in CodY activity (i.e., genes in cluster 1) achieved, on average, complete de-repression in the R61K mutant, whereas those genes least sensitive to changes in CodY activity (i.e., genes in cluster 4) showed >50% expression in the G129D mutant. Genes crossed the 50% threshold in the R61H and R61E mutants for clusters 2 and 3, respectively. In general, metabolic and virulence genes were dispersed throughout each cluster (**Dataset S3, Fig. S3B**, compare grey vs. black lines) and genes either co-transcribed or sharing a biological function fell into the same cluster (**Dataset S3**). For example, the majority of the purine biosynthesis genes (i.e., *purCSQLFMHD*) fell into cluster 2; *purEK* fell into cluster 3. Genes for heme-based iron acquisition (*isdCDE*), genes of the *agr* RNAII transcript (*agrBDCA*) and the majority of the ILV biosynthetic genes (*ilvDBHC, leuABCD, ilvA*) all fell into cluster 3; *hld* (delta toxin; *agr* RNAIII transcript), the unlinked ILV biosynthetic gene *ilvE*, and the capsule biogenesis genes (*cap5ABCDEFGHIJK*) all fell into cluster 4. Moreover, positively-regulated enterotoxin-like protein genes (i.e., *eto1-6*) and genes of the accessory Sec locus (i.e., *asp1-3* and *secY*) fell into cluster 5.

Genes for amino acid uptake are sensitive to changes in CodY activity

Analysis of the *k*-means clustering revealed that nutrient uptake and biosynthesis are separated along the ILV gradient. We focused our analysis on transport systems shown or believed to salvage available branched-chain amino acids (i.e., ILV; *brnQ1, brnQ2;* QV15_00670, QV15_01265), methionine (*metNIQ2;* QV15_04055-04065) and histidine (QV15_01335), as well as genes that direct the synthesis of these amino acids (*ilv-leu;*

metICHE, mdh; hisZGDC$_2$HAFIE) because they have been previously characterized (Burke & Pattee, 1972, Kaiser *et al.*, 2015, Majerczyk *et al.*, 2010, Rodionov *et al.*, 2004, Schoenfelder *et al.*, 2013). We consistently observed that ILV, histidine and methionine uptake genes were relatively sensitive to changes in CodY activity compared to their cognate biosynthesis genes, falling into clusters 2, 2 and 1, respectively (**Dataset S3**, **Fig. 2**). A notable exception is a duplicate set of putative methionine uptake genes (*metNIQ1;* QV15_01935-01945) that fall into cluster 3 that are relatively resistant to changes in CodY activity. In contrast, biosynthetic genes for ILV, histidine and methionine fell into clusters 3 and 4, 3 and 2, respectively. Interestingly, genes encoding enzymes and proteins for the synthesis of aromatic amino acids (*trp, aro, tyr*), lysine (*lys, dap, asd*) and methionine are more sensitive to changes in CodY activity than those genes for ILV and histidine synthesis and fall into cluster 2 (**Dataset S3**, **Fig 3A**).

To determine the extent to which these changes in CodY-dependent gene expression alter the steady state levels of these amino acids and their intermediates, we quantified steady-state intracellular abundances using targeted tandem liquid chromatography-TOF MS (LC-MS) analysis of cell lysates during exponential phase in TSB. Samples were collected within one generation of those collected for gene expression analysis. Consistent with our RNA-Seq results, we observed an increase in intracellular threonine in the *codY* null mutant relative to UAMS-1 (**Fig. 4A**; $p < 0.05$). Isoleucine and leucine, though not resolved in our mobile phase, were also significantly increased. Aspartate and acetyl homoserine (methionine biosynthetic intermediate) pools were reduced in the *codY* null mutant relative to UAMS-1, reflecting their use in biosynthesis (**Fig. 4**; $p < 0.05$). As CodY activity was reduced, we observed small, but dose-dependent changes in these metabolite abundances across our collection of strains (**Fig. 4A**). We also measured significant increases in intracellular serine pools as well as significant decreases in proline and pyrrole carboxylate as CodY activity decreased. A full list of compounds analyzed and the statistical significance of their changes is available in the *Supporting Information* (**Dataset S4**).

Reductions in CodY activity result in increases in static biofilm development

To determine whether sequential regulation of CodY gene targets leads to detectable changes in protein production and behavior, we examined two well characterized in vitro phenotypes – static biofilm formation and the production of thermonuclease, whose activity is required for the development of biofilms under flow conditions (Kiedrowski *et al.*, 2011, Moormeier *et al.*, 2014). CodY-deficient strains of UAMS-1 have been shown to form thicker biofilms relative to UAMS-1; this has been attributed to the production of PIA due to de-repression of the *ica* locus (Atwood *et al.*, 2015, Majerczyk *et al.*, 2010, Majerczyk *et al.*, 2008). Our RNA-Seq data and static biofilm assays confirm the entire *ica* locus (*icaADBC;* except the divergently-transcribed regulator *icaR*) is over-expressed 37- to 225-fold in the *codY* null mutant (**Dataset S1**) and the *codY* null mutant forms significantly more biofilm relative to the wild-type parent strain (**Fig. 5A**, compare UAMS-1 vs. *codY*). We used a *sarA* mutant to confirm we had removed the majority of non-adherent cells because of its known defect in biofilm development (Beenken *et al.*, 2003). Interestingly, we saw no statistical difference relative to UAMS-1 in static biofilm development when we deleted the *ica* locus in otherwise wild-type cells. However, CodY-deficient cells formed relatively little static

biofilm when also lacking an intact *ica* locus, providing the most convincing genetic evidence to date for a PIA-dependent biofilm when CodY is inactive in UAMS-1 (**Fig. 5A**, compare UAMS-1 vs. *ica* and *ica* vs. *ica codY*).

ica gene expression is regulated by the *icaR* transcriptional repressor (Jefferson *et al.*, 2004). To determine whether CodY regulates *icaADBC* gene expression through IcaR, we constructed *icaR, codY,* and *icaR codY* double mutants and measured transcript abundance of *icaA* using qRT-PCR. In UAMS-1 and the *icaR* single mutant, *icaA* transcript abundance was extremely low and indistinguishable from our no-reverse transcriptase control (**Fig 6A**). *icaA* was > 60-fold overexpressed in the *codY* null mutant; in the *icaR codY* double mutant, *icaA* transcript was essentially unchanged (**Fig 6A**). Whereas UAMS-1 and the *icaR* null mutant both formed relatively little static biofilm (crystal violet absorbance < 1), the *codY icaR* double mutant formed ~3-fold more biofilm than the *codY* single mutant (**Fig 6B**). From these experiments, we conclude that CodY is epistatic to IcaR.

The *icaADBC* genes fall into cluster 4, indicating that expression of these genes is relatively robust to changes in CodY activity (**Dataset S3**, **Fig. 5B**). This suggested that the thickest PIA biofilms would be produced when CodY activity is eliminated. To answer this question, we measured the ability of our strains producing variable CodY activity to form a biofilm and found that the $CodY^{R61K}$, $CodY^{R61H}$ and $CodY^{R61E}$ variant-producing strains show a two- to three-fold increase in biofilm formation, whereas biofilm formation was maximal in both the $CodY^{G129D}$ variant-producing strain and the CodY-deficient strain (**Fig. 6C**). Taken together, our results indicate UAMS-1 produces an *ica*- and PIA-dependent biofilm when CodY is inactive, and that although *ica* expression is turned on under conditions that mimic relatively severe ILV depletion, small changes in *ica* expression appear to trigger biofilm formation.

CodY controls secreted nuclease production by grading saePQRS *expression*

nuc, coding for thermonuclease, is directly controlled by the SaePQRS two-component system (TCS) and is a CodY-regulated virulence factor (Majerczyk *et al.*, 2010, Olson *et al.*, 2013). The *nuc* locus is ~22-fold de-repressed in the *codY* null mutant relative to UAMS-1 (**Dataset S1**), but regulation of *nuc* by CodY is likely to be indirect, as no obvious CodY motif was detected in or near the *nuc* promoter region (Majerczyk *et al.*, 2010). We did, however, measure an approximate three- to eight-fold increase in *saePQRS* expression in the *codY* null mutant (**Dataset S1**). In order to determine whether CodY regulates *nuc* expression *via* the SaeRS TCS, we performed an epistasis experiment and measured *nuc* transcript abundance in exponentially growing *S. aureus* cells. Consistent with our RNA-Seq data, we saw a ~50-fold increase in *nuc* expression when we knocked out *codY* (**Fig. 7A**). In a *codY saeR* double mutant, expression of *nuc* was ablated, indicating that SaeR is required for *nuc* overexpression in a *codY* null mutant (**Fig. 7A**, compare *codY* vs. *codY saeR*). To determine whether the effect of CodY is specific to UAMS-1, we repeated the experiment in a community-acquired MRSA isolate (LAC, USA300 lineage) (Voyich *et al.*, 2005) and found that again, overexpression of *nuc* in a CodY mutant requires an intact *sae* locus (**Fig. 7B**).

Interestingly, *saePQR* (cluster 3) and *saeS* (cluster 2) respond to moderate changes in CodY activity, whereas *nuc* (cluster 4) is de-repressed only when CodY activity is substantially reduced (**Fig. 7C**). To determine whether the increases in *nuc* expression in the *codY* mutant strains lead to increased secretion of thermonuclease enzyme, we used a FRET-based assay to quantify nuclease present in culture supernatants (Kiedrowski *et al.*, 2011). During exponential growth in TSB, we detected 1.5 units (U) ml^{-1} $OD_{600}{}^{-1}$of thermonuclease activity in UAMS-1 culture supernatants. In contrast, the *codY* null mutant accumulated 14.3 U ml^{-1} $OD_{600}{}^{-1}$ of thermonuclease activity in culture supernatants (**Fig. 8A**, compare UAMS-1 versus *codY*). This activity is approximately 50% of the activity measured in *sarA* culture supernatants known to overproduce thermonuclease (Kiedrowski *et al.*, 2011); as expected, culture supernatants of a strain lacking *nuc* showed no secreted nuclease activity (**Fig. 8B**). We found coinciding trends when comparing nuclease activity, *nuc* transcript numbers, and *nuc* RNA-Seq counts, indicating that rising levels of *saePQRS* and *nuc* transcripts lead to increases in secreted nuclease as CodY activity is reduced (**Figs. 7**, **8**; **Dataset S1**, **Table 2**). Taken together, these results show that CodY represses the expression and production of thermonuclease during rapid, exponential growth, and this graded regulation is dependent on the Sae TCS.

Discussion

Gram-positive bacteria like *S. aureus* are metabolically versatile, can reside in and on human hosts as commensal bacteria, and as opportunistic pathogens, can cause life-threatening infections. A complex network of regulatory factors adjusts gene expression and physiology to ensure survival and promote multiplication in diverse environments. To that end, transcription factors that bind key intracellular metabolites can regulate many genes simultaneously, mediating, at least in part, the shift between commensal and pathogenic lifestyles. Despite observations that the expression of the most important virulence genes often correlates with the exhaustion of available nutrients (Somerville & Proctor, 2009), there is limited knowledge of how the signaling of nutrient status and the resulting physiological responses are coordinated. While the targets of CodY are known in *S. aureus*, virtually nothing is known about the threshold levels of CodY activity required to regulate each CodY-controlled gene. The ILV binding pocket in *B. subtilis* has been characterized (Villapakkam *et al.*, 2009) and is highly similar to that of *S. aureus.* Using available structural data from the *B. subtilis* CodY protein, we sought to modulate the activity of *S. aureus* CodY by constructing a collection of strains that produce CodY proteins with varying amounts of residual regulatory activity. This approach allows us to simulate an ILV limitation while growing all cells under identical conditions where the only variable is CodY activity. We report the first linkage of turning on and off metabolism and virulence gene expression to increasing nutrient depletion, revealing non-binary modulation of a regulon built to mediate adaptation to dynamic environments.

CodY directs the metabolism of key nutrients sequentially along an ILV gradient

Our data suggest that *S. aureus* uses CodY to prioritize nutrient uptake and biosynthesis during growth in a complex mixture of carbon and nitrogen sources and generally, uptake genes are more sensitive to changes in CodY activity than their cognate biosynthetic

pathways. Such a strategy makes physiological sense and allows the bacterium to scavenge available nutrients before diverting carbon, nitrogen and energy to their biosynthesis. Interestingly, while one set of uptake genes was de-repressed with a relatively small change in CodY activity, another putative set of methionine uptake genes, *metNIQ1* (QV15_01935-01945) fell into in cluster 3 and is turned on at a lower level of CodY activity required to turn on methionine biosynthesis (**Fig. 2C**). Although these uptake systems have not been biochemically characterized, we speculate that they may differ in affinity as is the case for ILV uptake proteins (Kaiser *et al.*, 2015), and our data potentially reveal a strategy in which a low-affinity system may be rapidly turned on to import relatively abundant methionine. As amino acids including methionine become increasingly scarce, a high-affinity uptake system may be induced along with the genes for methionine synthesis.

We found that not all synthesis pathways are regulated at the same level of residual CodY activity. First, aromatic amino acid biosynthetic genes are turned on at a lower threshold CodY activity compared to other amino acid biosynthetic genes (cluster 2). Histidine (synthesized via *his*; cluster 3) is known to act post-transcriptionally to cross-regulate aromatic amino acid synthesis in *B. subtilis* (**Fig. 3B**) (Kane & Jensen, 1970, Nester, 1968). Thus, *S. aureus* may prioritize aromatic amino acid synthesis to avoid negative cross-pathway regulation by rising histidine levels to maintain a steady pool of aromatic amino acids for protein production as well as for folic acid and ubiquinone synthesis. Second, although lysine, methionine, threonine and, by extension, isoleucine, are all synthesized from aspartate and are collectively known as the aspartate family of amino acids (**Fig. 4B**) (Paulus, 1993), we consistently saw lysine and methionine biosynthetic genes turned on with relatively minor reductions in CodY activity (cluster 2) compared to threonine and ILV biosynthetic genes (cluster 3). Because *S. aureus* uses lysine to synthesize peptidoglycan (Mengin-Lecreulx *et al.*, 1999, Schleifer & Kandler, 1972), it is possible that *S. aureus* prioritizes lysine synthesis to support both peptidoglycan synthesis and protein production even when pools of amino acids are only slightly reduced. Because methionine is limited in physiological fluids and undetectable in nasal secretions at the site of commensal carriage (Basavanna *et al.*, 2013, Krismer *et al.*, 2014), the positions of the *met* biosynthetic genes within the overall CodY expression hierarchy may reflect the adaption of *S. aureus* to the human host and the need to synthesize this amino acid.

As gene annotations improve and biochemical data regarding biosynthetic and degradative pathways become increasingly available, our metabolite data can be further mined for physiological significance. For example, the genes responsible for conversion of threonine to serine via glycine (SAR1326 and *glyA* [SAR2201]) were not differentially expressed between the wild type and *codY* null mutant strains. However, serine was > 6-fold more abundant in the *codY* null mutant compared to wild type cells ($p < 0.05$). It has been suggested that serine can be synthesized from 3-phosphoglycerate (Lee *et al.*, 2009b). *serA* (SAR1801; coding for 3-phosphoglycerate dehydrogenase) is overexpressed 80-fold in the *codY* null mutant, but genes encoding the phosphoserine transaminase and phosphatase appear to be absent in UAMS-1. At this time we cannot rule out the possibility for increased serine transport or synthesis via an uncharacterized pathway.

We note here that our data reflect steady state abundances and only suggest altered fluxes through a particular pathway; in the future, use of isotopic labeling can provide information regarding carbon and nitrogen flow. Though not significant, we detected a trend toward increasing homocysteine and decreasing S-adenosylmethionine (SAM) as CodY activity decreased; our methods did not allow for reliable detection of redox-labile cysteine. These observations are consistent with the upregulation of genes for methionine synthesis via aspartate (**Fig 4**). Cysteine synthesis can proceed via a dedicated pathway and, in some bacteria including *B. subtilis,* the reverse transsulfuration pathway whereby methionine is converted to cysteine via homocysteine and the SAM recycling pathway (Rodionov *et al.*, 2004). Based on our data, we have no evidence for altered regulation of the reverse transsulfuration pathway.

CodY links biofilm development to nutrient availability

The effect of a *codY* null mutation on biofilm formation in UAMS-1 was documented previously; CodY-deficient cells behave as though nutrients are completely exhausted. Our genetic analysis of *ica* operon regulation suggests that CodY is epistatic to IcaR. That is, during exponential growth, there is no effect of disrupting *icaR* (**Fig. 6**). This is likely because CodY is active and represses transcription by binding to a site internal to *icaB* (Majerczyk *et al.*, 2010); however, we were unable to measure a quantitative difference between *icaB* transcript abundance upstream or downstream of the binding site (data not shown). Interestingly, though there is a trend toward an increase in expression, we see no significant up-regulation of *ica* when we measure *icaA* transcript abundance in the *icaR codY* double mutant relative to the *codY* single mutant. It is possible that this increase is responsible for the 3-fold increase in static biofilm production. Alternatively, there may be additional transcriptional or post-transcriptional regulation. For example, the 3’ untranslated region (3’-UTR) of *icaR* contains an element that base pairs with the Shine-Delgarno region of the *icaR* messenger RNA, regulating *icaR* translation and IcaR abundance (Ruiz de los Mozos *et al.*, 2013). The environmental signals or factors that control this regulation are unknown but may include nutrient availability and/or CodY. This could also explain the mild increase in biofilm formed in the strains producing the R61K and R61H variants of CodY (**Fig 5C**) despite no apparent change in *ica* expression. The exact mechanism for CodY-mediated repression of *ica* is unclear, but given the position of the CodY binding site, may involve a roadblock mechanism (Belitsky & Sonenshein, 2011). This is under investigation in our lab.

We found that the *ica* deletion mutant shows no detectable biofilm phenotype after 24 h (**Fig. 6**), suggesting that the mild biofilm produced by UAMS-1 under static biofilm conditions is PIA-independent. However, PIA accumulates during exponential growth and, after the transition to post-exponential and stationary phases, carbon is directed to capsule synthesis, which shares the same precursors (Sadykov *et al.*, 2010, Majerczyk *et al.*, 2008). This is also in good agreement with the fact that CodY represses capsule biosynthesis genes during exponential phase ((Majerczyk *et al.*, 2010), **Dataset S1**). Thus, we are hesitant to say that UAMS-1 biofilms are completely PIA-independent. Alternatively, our ILV titration and nutrient exhaustion experiments are consistent with the notion that nutrients must be severely depleted before genes within clusters 3 and 4 are de-repressed (**Table 1**, **Fig. 1**).

icaADBC are among those genes relatively insensitive to changes in CodY activity (cluster 4). Thus, CodY activity may remain sufficiently high to repress the *ica* locus in the UAMS-1 wild type strain and prevent the production of a biofilm. Deletion of the *ica* locus in a *codY* null mutant eliminates the hyper-biofilm phenotype observed in the *codY* null mutant and in fact these cells fail to produce biofilms to the extent measured in UAMS-1 (**Fig. 6**). This phenotype is reminiscent of *fnbAB* strains of USA300 LAC that fail to produce appreciable amounts of PIA and fail to form significant biofilm (Atwood *et al.*, 2015, McCourt *et al.*, 2014). Thus, in strains other than UAMS-1, cell attachment and biofilm development are likely synchronized with nutrient availability.

In UAMS-1, *codY* null mutants produce PIA-dependent biofilms but the biofilm yields measured in our variant strains were stepwise in nature and did not follow a smooth increase in the mutants that might have been predicted by the *ica* gene expression patterns alone (**Figs. 6B, C**). We propose that UAMS-1 produces PIA-dependent biofilms as CodY activity drops. However, at a critical threshold level of CodY activity, biofilm development is restricted (**Fig. 6C**). We postulate this is due to CodY-dependent, sequential de-repression of genes whose products have been shown to be important for remodeling the *S. aureus* biofilms (Kiedrowski *et al.*, 2011, Moormeier *et al.*, 2014, Mootz *et al.*, 2013). For example, CodY controls the expression of the protease genes *sspA, sspB, sspC* and *aur,* and thermonuclease *nuc.* These genes are 3- to 44-fold regulated by CodY and are relatively insensitive to changes in CodY activity (**Datasets S1, S3**; clusters 3 and 4). As nutrients continue to be depleted, CodY is further inactivated and PIA production may override the effect of nucleases and proteases. Interestingly, it has been proposed that biofilm towers are important for surviving environmental stress, and gene expression in microfluidic devices has revealed biofilm towers contain metabolically distinct microniches (Moormeier *et al.*, 2013). Because nutrients likely diffuse poorly into biofilms and because CodY controls metabolic and virulence gene expression, it is tempting to speculate that CodY is responsible, at least in part, for distinct patterns of gene expression and subsequent regions of cells with specific roles. An examination of biofilm development under biologically relevant flow where nutrients are replenished over time is underway and will enable us to more clearly define CodY's role in sculpting staphylococcal biofilms.

CodY instigates cascading virulence factor regulation

In *S. aureus*, CodY has been shown to control the expression of virulence genes directly by binding to sites containing a CodY motif and indirectly by controlling the expression of *agr* (Majerczyk *et al.*, 2010, Majerczyk *et al.*, 2008, Pohl *et al.*, 2009). Additionally, Majerczyk *et al.* identified *saeRS* to be regulated by CodY (Majerczyk *et al.*, 2010). However, the dynamics of this regulation have remained unexplored. We document the first example of cascading regulation of virulence genes by CodY in *S. aureus* by demonstrating CodY grades *sae* expression under conditions that mimic ILV depletion to induce *nuc* expression. The positions of *saePQRS* (clusters 2 and 3) and *nuc* (cluster 4) within the CodY expression hierarchy reveal that the threshold for *saePQRS* induction is lower than for *nuc* regulation. That is, *saePQRS* expression precedes *nuc* expression (**Fig. 7C**). The *sae* P1 promoter is activated by *agr,* and repressed by Rot and the alternative sigma factor SigB, each of which is effected by CodY (Geisinger *et al.*, 2006, Li & Cheung, 2008, Majerczyk *et al.*, 2010,

Novick & Jiang, 2003, Pohl *et al.*, 2009), suggesting regulation by CodY is indirect. Interestingly, it has been proposed that the ratio of activated SaeR (SaeR~P) relative to SaeR rather than absolute abundance of SaeR dictates target gene transcription. *coa* and *hla,* regulated by CodY and targets of SaeR, showed no increase in expression during exponential and post-exponential phases when *saeR* was placed under the control of an inducible promoter (Mainiero *et al.*, 2010). Under these conditions, CodY is active and likely masks expression of these targets as SaeR~P increases. We propose that nutrient availability, monitored by CodY, ensures precise dosing and timing of Sae-dependent gene expression. This is in agreement with the notion put forth by Novick and Jiang whereby the *sae* locus collects converging environmental and population density signals to adjust gene expression (Novick & Jiang, 2003). Precisely how CodY controls the expression and activity of the Sae TCS is under investigation in our laboratory.

Staphylococcus aureus uses graded CodY activity to modulate metabolism and virulence gene expression in vitro

In this report, we used strains producing variable CodY activity to pinpoint the threshold activities required to regulate each metabolic and virulence gene, offering snapshots of transcript abundance at discrete points along the CodY activity continuum. Changes in transcript abundance of selected CodY targets in these strains mirror changes seen when wild-type cells are grown in defined medium with varying concentrations of exogenous ILV. For example, *ilvD* (cluster 3) is de-repressed at a lower CodY activity threshold than *hld* (cluster 4); when grown in medium containing 15 μM ILV, *ilvD* was completely de-repressed while *hld* exhibited only ~10% of the expression observed in the *codY* null mutant. These experiments should be interpreted with caution, as medium- and growth-rate dependent effects can confound the analysis. Indeed, at low ILV concentrations, the doubling time of *S. aureus* strains increases ~2-fold (**Table 1**). As the intracellular pools of ILV and guanine nucleotides drop during nutrient depletion, the active fraction of CodY decreases. If one considers nutrient sufficiency as the moment prior to limitation, our use of partial CodY activity variants can serve as a surrogate to our initial time course experiment (**Fig 1**). Indeed, based on our results, CodY gene targets can be arranged into temporal classes with clear “early” and “late” gene expression (**Fig. S3**, **Fig. 9, Dataset S3**). Such a classification is consistent with the sensitivity of selective gene targets to changes in CodY activity (**Fig. S1)**. For example, *S. aureus* generally turns on nutrient uptake before devoting carbon, nitrogen and energy to biosynthesis, whose genes are turned on relatively late when nutrients are nearly depleted. Genes coding for proteins and enzymes for utilizing other carbon and nitrogen sources are turned on and off at various points along the ILV gradient. For instance, transporters for oligopeptides (QV15_04450-04470), *p*-aminobenzoyl-glutamate (QV15_12780), and galactitol (QV15_00960) are turned on early. *pycA* (QV15_05170), *sucA* (QV15_06885) and QV15_00370, coding for pyruvate carboxylase, 2-oxoglutarate dehydrogenase and acetoin reductase - all of which control the distribution of pyruvate and 2-oxoglutarate - are also turned on early. In contrast, a transporter for trehalose (*treP*, QV15_02000) and *ldh* (QV15_13410; coding for lactate dehydrogenase) are turned on late, suggesting that trehalose and lactate are utilized after other nutrients are exhausted. QV15_04760, coding for an Fe^{3+} transport protein and QV15_11350-11355, coding for the

anabolic acetolactate decarboxylase and synthase *alsDS* are positively regulated by CodY and are turned off as nutrients are depleted.

Most revealing in this experiment is the placement of many of the well-studied virulence genes within the CodY-dependent gene expression hierarchy in *S. aureus,* linking the availability of nutrients to the ability to cause disease (**Fig. 9**). In our working model, during periods of relative nutrient abundance, positively regulated genes coding for microbial surface components recognizing adhesive matrix molecule (MSCRAMM) proteins like *fnbA, spa, clfB* and *sdrC* are expressed as are genes encoding 8 of the 29 enterotoxin-like proteins located within the same genomic context as the *egc* cluster (Thomas *et al.*, 2006). These genes are among the first to be shut off as ILV and GTP are depleted. Although the enterotoxic properties have not been confirmed, one possibility is that *S. aureus* may attempt to prevent eliciting an immune response as a survival strategy once nutrients become limiting. MSCRAMM proteins are shut off upon nutrient limitation to potentially limit persistence and promote dissemination. As nutrients continue to be depleted, *sae* as well as genes coding for a type VII secretion system (*esa*) and *chp* are turned on. *agr* and genes coding for enzymes and proteins that extract nutrients from tissue (e.g., lipases, proteases, hyaluronidase) and those that elicit cellular toxicity (e.g., *hld*) are among the last genes to be de-repressed, suggesting that *S. aureus* limits the most severe damage to the host until nutrients are nearly depleted.

Hosts often sequester essential nutrients that challenge bacteria to adjust gene expression to nutrient limiting environments (Weinberg, 1975). Moreover, reactive oxygen species serve as an additional host defense and can damage essential iron-sulfur clusters in IlvD and LeuD (Jang & Imlay, 2007, Brown *et al.*, 1995), potentially rendering *S. aureus* an ILV auxotroph during infection. Human plasma and ocular fluids contain millimolar concentrations of ILV, but anterior nares contain 10-fold lower concentrations of leucine and valine and lack detectable isoleucine (Durham, 1970, Nasset *et al.*, 1979, Krismer *et al.*, 2014, Nakatsukasa *et al.*, 2011). Moreover, staphylococcal abscesses have been proposed to be limiting in guanine nucleotides (Valentino *et al.*, 2014). Thus, *S. aureus* likely encounters varying levels of ILV and guanine nucleotides in host tissue during infection, potentially resulting in variable CodY activity and CodY-dependent gene expression in various host niches. A recent study showed that community-acquired *S. aureus* (CA-MRSA) strains lacking CodY are hypervirulent in two mouse models of infection, demonstrating that CodY regulates virulence gene expression *in vivo* (Montgomery *et al.*, 2012). However, the extent to which CodY is active in these infection sites is unknown. Indeed, CodY may serve as an important regulator whose graded activity can mediate the switch between commensal and pathogenic lifestyles. We are actively pursuing these questions in our laboratory.

Experimental Procedures

Strains and growth conditions

Bacterial strains used in this study are listed in **Tables 3** and **S1**. Lennox (L) medium lacking glucose (Lennox, 1955) was used to cultivate *Escherichia coli* strains; tryptic soy broth (TSB) or chemically defined medium (CDM) (Hussain *et al.*, 1991) was used to cultivate *S. aureus* strains. When necessary, media were solidified with agar at 1.5% [w/v]. Media were

supplemented with antibiotics at the following concentrations to maintain selection: ampicillin (Ap), 50 μg ml^{-1}; chloramphenicol (Cm), 10 μg ml^{-1}; erythromycin (Em), 5 μg ml^{-1}; tetracycline (Tc), 1.5 μg ml^{-1}. 5-bromo-4-chloro-3-indolyl-beta-D-galacto-pyranoside (X-gal) was included at a concentration of 80 μg ml^{-1} to detect BgaB activity on solid media. Experiments were performed in 125 ml or 250 ml DeLong shake flasks with either 25 ml or 50 ml culture volumes, respectively (5:1 flask-to-volume ratio). Experiments were initiated by inoculating overnight cultures incubated in TSB at 37°C to an optical density at 600 nm (OD_{600}) of 0.05. Flasks were incubated at 37°C in an Innovo orbital shaking water bath (New Brunswick) with vigorous shaking (280 RPM) until OD_{600} ~1.0. In order to dilute out the effect on transcription of residual quorum-sensing signals accumulated during overnight growth (e.g., RNAIII), cultures were re-diluted into fresh medium to OD_{600} = 0.05, maintaining the flask-to-volume ratio. Growth was monitored as increase in absorbance at 600 nm using a Beckman DU350 UV-visible spectrophotometer (Beckman Coulter).

Molecular biology and genetic techniques

Oligonucleotides used in this study were synthesized by Integrated DNA Technologies (Coralville, IA). Non-radioactive Sanger sequencing was performed by GeneWiz (Germantown, MD). Plasmids were introduced into *S. aureus* strain RN4220 by electroporation as previously described (Schenk & Laddaga, 1992). Plasmids and marked mutations were mobilized between *S. aureus* strains by φ11-mediated transduction (Novick, 1991).

Strain and plasmid construction

Fragments for generating mutant alleles were synthesized using overlap PCR (Vallejo *et al.*, 2008) using oligonucleotides in **Table S2**. Mutant strains producing variant CodY proteins or deleted for *ilvE* or *sucD* were constructed by allelic exchange using pMAD and confirmed by sequencing (Arnaud *et al.*, 2004). When possible, mutants were reconstructed in UAMS-1 by transduction. The mutant producing $CodY^{G129D}$ (encoded by the *codY489* allele) was isolated as a spontaneous mutant during the construction of an *ilvE* null mutant. We moved the *codY489* allele into UAMS-1 by cotransduction with a linked $sucD^{+}$ allele into a *sucD::cat194* mutant, selecting for growth on chemically defined medium (Lee *et al.*, 2009a) lacking glucose as the carbon source.

codY and *saeR* mutant construction

S. aureus JE2 containing transposon insertions in the *codY* gene and the *saeR* gene were obtained from the Nebraska Transposon Mutant Library (NTML, strains NE1555 and NE1622, respectively) (Fey *et al.*, 2013). The pTET plasmid from the NTML genetic toolkit was used to replace the erythromycin resistance cassette with a tetracycline-resistant cassette as previously described (Bose *et al.*, 2013). These mutations were then moved into UAMS-1 by transduction.

Generation of the *nuc-sGFP reporter fusion*

To generate the *nuc*-s*GFP* fusion, we used a double reporter shuttle vector designated as pMRSI (**Fig. S4**). The pMRSI plasmid, a derivative of pDM4 (Moormeier *et al.*, 2013), was constructed by PCR using primers KPPE-TIR-f and NNSB-TIR*-r to replace divergently transcribed *cidABC* and *lrgAB* promoter regions of the pDM4 with a *multiple cloning site (*MCS). Then, the PCR fragment was treated with the restriction endonuclease DpnI (to hydrolyze the pDM4 template DNA), self-ligated and transformed into the *E. coli* strain DH5α. The replacement of the *cidABC* and *lrgAB* promoter regions with the MCS and integrity of the TIRs and s*DsRed* and s*GFP* genes in the pMRSI plasmid were confirmed by DNA sequencing using primers sDsRed-S-r, sGFP-S-r, pCN51-S1-f, and pCN51-S-r.

Primers used for construction of the *nuc*-s*GFP* reporter fusion were generated based on the sequence of *S. aureus* strain MRSA252 (NC_002952.2). A 382-nucleotide (nt) PCR fragment containing the promoter region, ribosome binding site (RBS) and translation initiating codon (ATG) of the *S. aureus* UAMS-1 *nuc* (SAR0847) gene was amplified using primers SphI-Pnuc-f and Pnuc1-r1. Following digestion with the restriction endonuclease SphI the PCR product was used to replace the SphI-SmaI DNA fragment of the plasmid pMRSI containing s*DsRed* gene, MCS and translation initiating codon (ATG) of the s*GFP* gene. The resulting recombinant plasmid designated as pMRSI-nuc was transformed into strain RN4220 by electroporation and then introduced into UAMS-1 and UAMS-codY strains by phage Φ11-mediated transduction.

RNA sampling and preparation

Samples (4 ml) of exponentially-growing cultures were rapidly withdrawn from each flask, mixed by vortexing with an equal volume of 100% ethanol-acetone quench solution (1:1 [v/v], pre-chilled to −20°C) and immediately frozen on dry ice and stored at −80°C. Nucleic acids were extracted from cell pellets after washing twice with 0.5 ml TE buffer (10 mM Tris-Cl [pH 8], 1 mM EDTA) by mechanical disruption using a Precellys 24 homogenizer (Bertin Technologies) in 4 ml Trizol (Invitrogen) with three 30 sec pulses at 6,800 RPM with 1 min incubations on wet ice between pulses. RNAs were isolated from clarified cell lysates using the Direct-Zol kit (Zymo Research Corporation) as per the manufacturer's recommendations. Genomic DNA was reduced to mathematically insignificant levels from samples using the Turbo DNA-free DNase treatment and removal kit (Ambion) according to the manufacturer's "rigorous-treatment" instructions. Total RNA preparations were quantified using a computer-controlled NanoDrop ND-1000 spectrophotometer (Thermo Scientific) running quantification software version 3.1.0.

Quantitative, real-time RT-PCR

250 ng of total RNA from each sample was used as template to synthesize cDNA using the Protoscript first strand cDNA synthesis kit (NEB) and random primers as per the manufacturer's instructions. Parallel reactions lacking reverse transcriptase were used to control for any remaining residual DNA contamination. Quantitative PCR (qPCR) was performed using a C1000 thermal cycler fitted with a CFX96 detection module (Bio-Rad) and SsoAdvanced Universal SYBR Green Supermix (Bio-Rad). Oligonucleotides for qPCR (**Table S2)** were used at a concentration of 400 nM. The reaction mixture was incubated at

98°C for 2 min followed by thermal cycling between 98°C and 60°C. No-template and no-RT controls were run on each plate for each assay, and specificity of each amplification product was verified using dissociation curve analysis. Standard curves were generated from serial dilutions of chromosomal DNA spanning at least 6 orders of magnitude. All reactions proceeded within 90% to 110% efficiency, and data points lay within linear regression with correlation coefficients (r^2 values) >98%. Data are presented as copies of target transcript relative to copies of *rpoC* or *polC* transcript because expression was constant between strains and replicates.

Transcriptional profiling with RNA-Seq and analysis

RNA-Seq was performed on two independent biological replicates for each strain. An 8.6-μg sample of nucleic acid was depleted of DNA using the Turbo DNA-free kit (Ambion). RNA integrity was assessed using a 2100 Bioanalyzer and the RNA 6000 Pico kit (Agilent); samples exhibiting RNA Integrity Numbers > 8 were used for downstream applications. DNA-depleted RNAs (negative PCR amplification of *rpoC* after 25 cycles using oSRB239 and oSRB240) were then depleted of rRNA using the Ribo-Zero magnetic kit for Gram-positive bacteria (Illumina). When necessary, RNAs were concentrated using the RNA Clean & Concentrator-5 kit (Zymo Research Corporation). Samples containing < 3% 16s and 23s rRNA were used for library preparation. Libraries were constructed using the TruSeq Stranded mRNA Library Prep Kit (Illumina), and sequenced in a single, high-throughput flow cell lane with TruSeq V3 chemistry using an Illumina (HiSeq 2500) at the Tufts University Genomics Core Facility. Single-ended reads were filtered to retain reads ~ 50bp, which were then cleaned and aligned to the *S. aureus* UAMS-1 genome (GI:727808807) using BWA (Li & Durbin, 2009). Because the published UAMS-1 annotation is incomplete, we first annotated the UAMS-1 genome with a custom BLAST+ pipeline, obtaining the best match from the USA300_TCH1516 annotation for protein sequences. If that failed, we obtained the best match from the MRSA252 genome. Genes previously listed as hypothetical or missing from these two genomes were manually searched against the NCBI nr database to find probable homologs. Additional annotations for the USA300 and MRSA252 strains were obtained from KEGG (Kanehisa & Goto, 2000, Kanehisa *et al.*, 2014). These sequencing data have been deposited in the Sequence Read Archive of the National Center for Biotechnology (accession number **xxxxx**).

Using a counts table generated with HTSeq (Anders *et al.*, 2015) containing mapped fragments per gene, all subsequent analyses were performed in R. *DESeq2* (Love *et al.*, 2014) was used to determine differential expression and normalization. Normalized counts from *DESeq2* were converted to *R*eads *P*er *K*ilobase per *M*illion reads mapped to *O*pen Reading Frames (ORFs), or RPKMOs, and then converted to percentages of maximal expression (i.e., expression in the CodY null mutant for negatively regulated genes and expression in the WT for positively regulated genes). *K*-means clustering of the least and most active CodY variant strains was used to group similarly expressed genes. Virulence genes were manually annotated by referencing previous literature (Cheng *et al.*, 2011, Majerczyk *et al.*, 2010, Majerczyk *et al.*, 2008, Kobayashi *et al.*, 2011, Rogasch *et al.*, 2006).

Metabolite sampling and analysis

Cells for metabolite analysis were grown in TSB as described above. At OD_{600} ~0.5, a 13 ml sample of cells was collected via vacuum filtration on 0.2 μm nitrocellulose filters (Millipore) and washed with 5 ml ice cold PBS. Filters were quenched in Acetonitrile/Methanol/H2O (40:40:20) supplemented with 0.1 M formic acid on a bed of dry ice. Cells were mechanically disrupted with 0.1 mm zirconia beads in Precellys 24 homogenizer (Bertin Technologies) for four, 30 sec pulses at 6,000 rpm with a 2 min cooling period on dry ice in between pulses. Lysates were clarified by a 15 min centrifugation at 18,213 × *g* at −11° C. Residual peptide concentration was used to normalize for biomass in these samples and was quantified using the Micro BCA Protein Assay Kit (Pierce) according to manufacturer's instructions. Tandem liquid chromatography coupled to Time-Of-Flight mass spectrometry (LC-MS) was performed as described previously (Brinsmade *et al.*, 2014). Experiments were performed independently at least three times.

LC-MS data processing and analysis

To normalize samples by biomass, raw ion counts obtained from LC-MS analysis were divided by the residual peptide concentration of each sample. To correct for batch effects between samples, the average ion count for all metabolites within a sample was calculated. The average ion count for each sample was divided by the average ion count for the WT-1 sample to generate a ratio. The biomass-normalized ion counts for all metabolites within a sample were each divided by this ratio to yield a corrected ion count. For the comparison of WT *S. aureus* (SRB337) with the *codY* null mutant (SRB372), a Mann-Whitney U test was used to determine significant differences in intracellular abundance. To compare the significance of differences across all six strains, we used Cuzick's nonparametric test for trend (Cuzick, 1985). Statistical analyses were performed in either Microsoft Excel or StataSE 14 (StataCorp).

Measuring nuc *expression using a* nuc-gfp *transcriptional reporter*

Strains were cultivated as described above. At the indicated time point, samples were removed, washed twice with phosphate buffered saline (PBS) and re-suspended in PBS to remove background fluorescence from TSB medium. Fluorescence was measured using a computer-controlled Tecan Infinite F200 Pro plate reader (equipped with 485 nm and 535 nm excitation and emission filters, respectively) and i-control software (Ver. 1.11). GFP signal acquisition settings were kept constant: gain, 35%; flash number, 25; integration time, 20 μs; lag time, 0 μs; settle time, 0 ms. Relative fluorescence units (RFUs) were calculated by subtracting the fluorescence from SRB337 (UAMS-1, lacks GFP reporter) and dividing by OD_{600} to correct for cell density.

Secreted Nuclease activity assays

Secreted nuclease activity was quantified essentially as described previously employing a Fluorescence Resonance Energy Transfer (FRET) assay (Kiedrowski *et al.*, 2011). In short, cells were grown as described above; supernatants were sterilized using 0.22 μm Spin X filters (Corning) and mixed with the FRET substrate: a single-stranded 15-mer oligonucleotide with the 5' end modified with a Cy3 fluorophore and the 3' end modified

with BHQ2 quencher (**Table S2**). Fluorescence from cleaved substrate was measured using a computer-controlled Tecan Infinite F200 Pro plate reader (equipped with 535 (25) nm and 590 (20) nm excitation and emission filters, respectively) and Magellan software (Ver. 7.1). Nuclease activity was related to a standard activity curve generated with purified micrococcal nuclease enzyme (Worthington Biochemicals).

Static biofilm assays

Static biofilm development was assayed in tissue-culture treated microtiter plates as previously described (Loughran *et al.*, 2014), except that the well bottom geometry was round rather than flat. Briefly, 200µl of freshly prepared biofilm medium (BFM; TSB supplemented with 0.5 % [w/v] glucose and 3 % [w/v] NaCl) was distributed to wells of the microtiter plate. *S. aureus* strains were grown as described above, inoculating BFM to an initial optical density of 0.01 in a total volume of 200 µl. Plates were incubated statically for 24 hours at 37°C. All proceeding manipulations from this point were performed at room temperature. Medium and non-adherent bacteria were removed from the microtiter plate by gentle inversion; fluid was completely removed by tapping against absorbent paper. The wells were then washed four times with 200 µl of Phosphate Buffered Saline (PBS; Ambion) to remove non-adherent cells. The PBS was also removed by gentle blotting against absorbent paper. Washed biofilms were fixed with 200 µl 100% [v/v] ethanol for 20 min followed by staining with 200 µl 0.1% [w/v] crystal violet (in 12 % [v/v] ethanol) for 8 min. The crystal violet was decanted and the wells were again washed four times each with 200 µl of PBS. Plates were inverted and dried for 10 min, at which time crystal violet was eluted into 200 µl of 95% ethanol for 10 min. Absorbance (600 nm) of each sample well was measured using an Infinite F200 Pro plate reader (Tecan), controlled by the Magellan software. When necessary, samples were diluted to remain within the linear range of the plate reader.

Immunoblot analysis

Immunoblotting was performed as described (Brinsmade *et al.*, 2014) except that we incubated samples with lysostaphin (2 mg ml^{-1}) prior to sonication and rabbit anti-CodY antibody was applied at 1:3,000 dilution.

Statistical Significance

Unless otherwise specified, statistical significance for experimental data was determined using Games-Howell test (Games *et al.*, 1979) chosen for its robustness across data types for pairwise comparisons. Unless noted elsewhere, experimental data reported are the result of at least two independent replicates.

Supplementary Material

Refer to Web version on PubMed Central for supplementary material.

Acknowledgements

We thank Jeffrey Cavanaugh for advice on the nuclease activity assay, and Alex Horswill and Mark Smeltzer for the gift of strains. We also thank Abraham “Linc” Sonenshein and Boris Belitsky for helpful advice, as well as Agnès

Roux, Deepak Sharma, Kevin Mlynek, Kevin Craig and Nivedita Sengupta for technical assistance as well as Jennifer Fox and Matt Hamilton for advice on statistical approaches.

Funding Information

This work was funded in part by an NIH Pathway to Independence Award (grant GM099893) and faculty startup funds to SRB, as well as a Research Project Grant (grant GM042219) prior to work performed at Georgetown University. The funders had no role in study design, data collection and interpretation, or the decision to submit the work for publication.

References

Anders S, Pyl PT, Huber W. HTSeq--a Python framework to work with high-throughput sequencing data. Bioinformatics. 2015; 31:166–169. [PubMed: 25260700]

Arnaud M, Chastanet A, Débarbouillé M. New vector for efficient allelic replacement in naturally nontransformable, low-GC-content, gram-positive bacteria. Appl. Environ. Microbiol. 2004; 70:6887–6891. [PubMed: 15528558]

Atwood DN, Loughran AJ, Courtney AP, Anthony AC, Meeker DG, Spencer HJ, Gupta RK, Lee CY, Beenken KE, Smeltzer M. Comparative impact of diverse regulatory loci on *Staphylococcus aureus* biofilm formation. Microbiologyopen. 2015; 4:436–451. [PubMed: 25810138]

Basavanna S, Chimalapati S, Maqbool A, Rubbo B, Yuste J, Wilson RJ, Hosie A, Ogunniyi AD, Paton JC, Thomas G, Brown JS. The effects of methionine acquisition and synthesis on Streptococcus pneumoniae growth and virulence. PLoS One. 2013; 8:e49638. [PubMed: 23349662]

Beenken KE, Blevins JS, Smeltzer M. Mutation of *sarA* in *Staphylococcus aureus* limits biofilm formation. Infect Immun. 2003; 71:4206–4211. [PubMed: 12819120]

Belitsky BR, Sonenshein AL. Roadblock repression of transcription by *Bacillus subtilis* CodY. J Mol Biol. 2011; 411:729–743. [PubMed: 21699902]

Blevins JS, Beenken KE, Elasri MO, Hurlburt BK, Smeltzer MS. Strain-dependent differences in the regulatory roles of sarA and agr in *Staphylococcus aureus*. Infect immun. 2002; 70:470–480. [PubMed: 11796572]

Bose JL, Fey PD, Bayles KW. Genetic tools to enhance the study of gene function and regulation in Staphylococcus aureus. Appl Environ Microbiol. 2013; 79:2218–2224. [PubMed: 23354696]

Brinsmade S, Alexander E, Livny J, Stettner A, Segrè D, Rhee K, Sonenshein A. Hierarchical expression of genes controlled by the *Bacillus subtilis* global regulatory protein CodY. Proc Natl Acad Sci U S A. 2014; 111:8227–8232. [PubMed: 24843172]

Brown OR, Smyk-Randall E, Draczynska-Lusiak B, Fee JA. Dihydroxy-acid dehydratase, a [4Fe-4S] cluster-containing enzyme in *Escherichia coli*: effects of intracellular superoxide dismutase on its inactivation by oxidant stress. Arch Biochem Biophys. 1995; 319:10–22. [PubMed: 7771772]

Bubeck Wardenburg J, Patel R, Schneewind O. Surface proteins and exotoxins are required for the pathogenesis of *Staphylococcus aureus* pneumonia. Infect Immun. 2007; 75:1040–1044. [PubMed: 17101657]

Burke ME, Pattee PA. Histidine biosynthetic pathway in *Staphylococcus aureus*. Can J Microbiol. 1972; 18:569–576. [PubMed: 4555843]

Casewell M, Hill R. The carrier state: methicillin-resistant *Staphylococcus aureus*. J Antimicrob Chemother. 1986; 18(Suppl A):1–12. [PubMed: 3091562]

Cheng A, DeDent A, Schneewind O, Missiakas D. A play in four acts: *Staphylococcus aureus* abscess formation. Trends Microbiol. 2011; 19:225–232. [PubMed: 21353779]

Cheng A, Kim H, Burts M, Krausz T, Schneewind O, Missiakas D. Genetic requirements for *Staphylococcus aureus* abscess formation and persistence in host tissues. FASEB J. 2009; 23:3393–3404. [PubMed: 19525403]

Cheung A, Nishina K, Trotonda M, Tamber S. The SarA protein family of *Staphylococcus aureus*. Int J Biochem Cell Biol. 2008; 40:355–361. [PubMed: 18083623]

Cuzick J. A Wilcoxon-type test for trend. Stat Med. 1985; 4:87–90. [PubMed: 3992076]

den Hengst CD, van Hijum SAFT, Geurts JMW, Nauta A, Kok J, Kuipers OP. The *Lactococcus lactis* CodY regulon: identification of a conserved *cis*-regulatory element. J Biol Chem. 2005; 280:34332–34342. [PubMed: 16040604]

Durham D. Distribution of free amino acids in human intraocular fluids. Trans Am Ophthalmol Soc. 1970; 68:462–500. [PubMed: 5524215]

Fey PD, Endres JL, Yajjala VK, Widhelm TJ, Boissy RJ, Bose JL, Bayles KW. A genetic resource for rapid and comprehensive phenotype screening of nonessential *Staphylococcus aureus* genes. MBio. 2013; 4:e00537–00512. [PubMed: 23404398]

Fink, PS. Biosynthesis of the branched-chain amino acids. In: Sonenshein, AL.; Hoch, JA.; Losick, R., editors. *Bacillus subtilis* and Other Gram-Positive Bacteria. American Society for Microbiology; Washington, DC: 1993. p. 307-317.

Games PA, Keselman HJ, Clinch JJ. Tests for homogeneity of variance in factorial designs. Psychol Bull. 1979; 86:978–984.

Geisinger E, Adhikari RP, Jin R, Ross HF, Novick RP. Inhibition of *rot* translation by RNAIII, a key feature of *agr* function. Mol Microbiol. 2006; 61:1038–1048. [PubMed: 16879652]

Gillaspy A, Hickmon S, Skinner R, Thomas J, Nelson C, Smeltzer M. Role of the accessory gene regulator (*agr*) in pathogenesis of staphylococcal osteomyelitis. Infect Immun. 1995a; 63:3373–3380. [PubMed: 7642265]

Gillaspy AF, Hickmon SG, Skinner RA, Thomas JR, Nelson CL, Smeltzer MS. Role of the accessory gene regulator (*agr*) in pathogenesis of staphylococcal osteomyelitis. Infect. Immun. 1995b; 63:3373–3380. [PubMed: 7642265]

Giraudo A, Calzolari A, Cataldi A, Bogni C, Nagel R. The *sae* locus of *Staphylococcus aureus* encodes a two-component regulatory system. FEMS Microbiol Lett. 1999; 177:15–22. [PubMed: 10436918]

Herold B, Immergluck L, Maranan M, Lauderdale D, Gaskin R, Boyle-Vavra S, Leitch C, Daum R. Community-acquired methicillin-resistant *Staphylococcus aureus* in children with no identified predisposing risk. JAMA. 1998; 279:593–598. [PubMed: 9486753]

Hussain M, Hastings JG, White PJ. A chemically defined medium for slime production by coagulase-negative staphylococci. J Med Microbiol. 1991; 34:143–147. [PubMed: 2010904]

Jang S, Imlay JA. Micromolar intracellular hydrogen peroxide disrupts metabolism by damaging iron-sulfur enzymes. J. Biol. Chem. 2007; 282:929–937. [PubMed: 17102132]

Janzon L, Löfdahl S, Arvidson S. Identification and nucleotide sequence of the delta-lysin gene, hld, adjacent to the accessory gene regulator (agr) of *Staphylococcus aureus*. Mol Gen Genet. 1989; 219:480–485. [PubMed: 2622452]

Jefferson KK, Pier DB, Goldmann DA, Pier GB. The Teicoplanin-Associated Locus Regulator (TcaR) and the Intercellular Adhesin Locus Regulator (IcaR) Are Transcriptional Inhibitors of the *ica* Locus in *Staphylococcus aureus*. J Bacteriol. 2004; 186:2449–2456. [PubMed: 15060048]

Joshi G, Spontak J, Klapper D, Richardson A. Arginine catabolic mobile element encoded *speG* abrogates the unique hypersensitivity of *Staphylococcus aureus* to exogenous polyamines. Mol Microbiol. 2011; 82:9–20. [PubMed: 21902734]

Kaiser J, Omer S, Sheldon J, Welch I, Heinrichs D. Role of BrnQ1 and BrnQ2 in branched-chain amino acid transport and virulence in S*taphylococcus aureus*. Infect Immun. 2015; 83:1019–1029. [PubMed: 25547798]

Kane JF, Jensen RA. Metabolic interlock. The influence of histidine on tryptophan biosynthesis in *Bacillus subtilis*. J Biol Chem. 1970; 245:2384–2390. [PubMed: 4315152]

Kanehisa M, Goto S. KEGG: kyoto encyclopedia of genes and genomes. Nucleic Acids Res. 2000; 28:27–30. [PubMed: 10592173]

Kanehisa M, Goto S, Sato Y, Kawashima M, Furumichi M, Tanabe M. Data, information, knowledge and principle: back to metabolism in KEGG. Nucleic Acids Res. 2014; 42:D199–205. [PubMed: 24214961]

Kiedrowski M, Kavanaugh J, Malone C, Mootz J, Voyich J, Smeltzer M, Bayles K. Nuclease modulates biofilm formation in community-associated methicillin-resistant *Staphylococcus aureus*. PLoS One. 2011; 6:e26714. H. AR. [PubMed: 22096493]

Kobayashi SD, Malachowa N, Whitney AR, Braughton KR, Gardner DJ, Long D, Bubeck Wardenburg J, Schneewind O, Otto M, Deleo FR. Comparative analysis of USA300 virulence determinants in a rabbit model of skin and soft tissue infection. J Infect DIs. 2011; 204:937–941. [PubMed: 21849291]

Kreiswirth BN, Löfdahl S, Betley MJ, O'Reilly M, Schlievert PM, Bergdoll MS, Novick RP. The toxic shock syndrome exotoxin structural gene is not detectably transmitted by a prophage. Nature. 1983; 305:709–712. [PubMed: 6226876]

Krismer B, Liebeke M, Janek D, Nega M, Rautenberg M, Hornig G, Unger C, Weidenmaier C, Lalk M, Peschel A. Nutrient limitation governs *Staphylococcus aureus* metabolism and niche adaptation in the human nose. PLoS Pathog. 2014; 10:e1003862. [PubMed: 24453967]

Kropec A, Maira-Litran T, Jefferson KK, Grout M, Cramton SE, Götz F, Goldmann DA, Pier GB. Poly-N-acetylglucosamine production in *Staphylococcus aureus* is essential for virulence in murine models of systemic infection. Infect Immun. 2005; 73:6868–6876. [PubMed: 16177366]

Kumar N, David M, Boyle-Vavra S, Sieth J, Daum R. High *Staphylococcus aureus* colonization prevalence among patients with skin and soft tissue infections and controls in an urban emergency department. J Clin Microbiol. 2015; 53:810–815. [PubMed: 25540401]

Lee D-S, Burd H, Liu J, Almaas E, Wiest O, Barabási A-L, Oltavi ZN, Kapatral V. Comparative genome-scale metabolic reconstruction and flux balance analysis of multiple *Staphylococcus aureus* genomes identify novel antimicrobial drug targets. J Bacteriol. 2009a; 191:4015–4024. [PubMed: 19376871]

Lee DS, Burd H, Liu J, Almaas E, Wiest O, Barabási AL, Oltvai ZN, Kapatral V. Comparative genome-scale metabolic reconstruction and flux balance analysis of multiple *Staphylococcus aureus* genomes identify novel antimicrobial drug targets. J Bacteriol. 2009b; 191:4015–4024. [PubMed: 19376871]

Lennox ES. Transduction of linked genetic characters of the host by bacteriophage P1. Virology. 1955; 1:190–206. [PubMed: 13267987]

Levdikov VM, Blagova E, Colledge VL, Lebedev AA, Williamson DC, Sonenshein AL, Wilkinson AJ. Structural rearrangement accompanying ligand binding in the GAF domain of CodY from *Bacillus subtilis*. J Mol Biol. 2009; 390:1007–1018. [PubMed: 19500589]

Levdikov VM, Blagova E, Joseph P, Sonenshein AL, Wilkinson AJ. The structure of CodY, a GTP- and isoleucine-responsive regulator of stationary phase and virulence in Gram-positive bacteria. J Biol Chem. 2006; 281:11366–11373. [PubMed: 16488888]

Li D, Cheung A. Repression of *hla* by *rot* is dependent on *sae* in *Staphylococcus aureus*. Infect Immun. 2008; 76:1068–1075. [PubMed: 18174341]

Li H, Durbin R. Fast and accurate short read alignment with Burrows-Wheeler transform. Bioinformatics. 2009; 25:1754–1760. [PubMed: 19451168]

Loughran AJ, Atwood DN, Anthony AC, Harik NS, Spencer HJ, Beenken KE, Smeltzer MS. Impact of individual extracellular proteases on *Staphylococcus aureus* biofilm formation in diverse clinical isolates and their isogenic *sarA* mutants. Microbiologyopen. 2014; 3:897–909. [PubMed: 25257373]

Love MI, Huber W, Anders S. Moderated estimation of fold change and dispersion for RNA-seq data with DESeq2. Genome Biol. 2014; 15:550. [PubMed: 25516281]

Lowy F. *Staphylococcus aureus* infections. N Engl J Med. 1998; 339:520–532. [PubMed: 9709046]

Mainiero M, Goerke C, Geiger T, Gonser C, Herbert S, Wolz C. Differential target gene activation by the *Staphylococcus aureus* two-component system *saeRS*. J Bacteriol. 2010; 192:613–623. [PubMed: 19933357]

Majerczyk CD, Dunman PM, Luong TT, Lee CY, Sadykov MR, Somerville GA, Bodi K, Sonenshein AL. Direct targets of CodY in *Staphylococcus aureus*. J Bacteriol. 2010; 192:2861–2877. [PubMed: 20363936]

Majerczyk CD, Sadykov MR, Luong TT, Lee C, Somerville GA, Sonenshein AL. *Staphylococcus aureus* CodY negatively regulates virulence gene expression. J Bacteriol. 2008; 190:2257–2265. [PubMed: 18156263]

McCourt J, O'Halloran DP, McCarthy H, O'Gara JP, Geoghegan JA. Fibronectin-binding proteins are required for biofilm formation by community-associated methicillin-resistant *Staphylococcus aureus* strain LAC. FEMS Microbiol Lett. 2014; 353:157–164. [PubMed: 24628034]

McNamara PJ, Milligan-Monroe KC, Khalili S, Proctor RA. Identification, cloning, and initial characterization of rot, a locus encoding a regulator of virulence factor expression in *Staphylococcus aureus*. J Bacteriol. 2000; 182:3197–3203. [PubMed: 10809700]

Mengin-Lecreulx D, Falla T, Blanot D, van Heijenoort J, Adams DJ, Chopra I. Expression of the *Staphylococcus aureus* UDP-N-acetylmuramoyl-L-alanyl-D-glutamate:L-lysine ligase in *Escherichia coli* and effects on peptidoglycan biosynthesis and cell growth. J Bacteriol. 1999; 181:5909–5914. [PubMed: 10498701]

Montgomery CP, Boyle-Vavra S, Roux A, Ebine K, Sonenshein AL, Daum RS. CodY deletion enhances in vivo virulence of community-associated methicillin-resistant *Staphylococcus aureus* USA300. Infect Immun. 2012 Epub ahead of print.

Moormeier D, Endres J, Mann E, Sadykov M, Horswill A, Rice K, Fey P, Bayles K. Use of microfluidic technology to analyze gene expression during *Staphylococcus aureus* biofilm formation reveals distinct physiological niches. Appl Environ Microbiol. 2013; 79:3413–3424. [PubMed: 23524683]

Moormeier DE, Bose JL, Horswill AR, Bayles KW. Temporal and stochastic control of *Staphylococcus aureus* biofilm development. MBio. 2014; 5:e01341–01314. [PubMed: 25316695]

Mootz JM, Malone CL, Shaw LN, Horswill AR. Staphopains modulate *Staphylococcus aureus* biofilm integrity. Infect Immun. 2013; 81:3227–3238. [PubMed: 23798534]

Naimi T, LeDell K, Como-Sabetti K, Borchardt S, Boxrud D, Etienne J, Johnson S, Vandenesch F, Fridkin S, O'Boyle C, Danila R, Lynfield R. Comparison of community- and health care-associated methicillin-resistant *Staphylococcus aureus* infection. JAMA. 2003; 290:2976–2984. [PubMed: 14665659]

Nakatsukasa M, Sotozono C, Shimbo K, Ono N, Miyano H, Okano A, Hamuro J, Kinoshita S. Amino Acid profiles in human tear fluids analyzed by high-performance liquid chromatography and electrospray ionization tandem mass spectrometry. Am J Ophthalmol. 2011; 151:799–808. [PubMed: 21310375]

Nasset ES, Heald FP, Calloway DH, Margen S, Schneeman P. Amino acids in human blood plasma after single meals of meat, oil, sucrose and whiskey. J Nutr. 1979; 109:621–630. [PubMed: 571014]

Nester EW. Cross pathway regulation: effect of histidine on the synthesis and activity of enzymes of aromatic acid biosynthesis in *Bacillus subtilis*. J Bacteriol. 1968; 96:1649–1657. [PubMed: 4973127]

Noble W, Valkenburg H, Wolters C. Carriage of *Staphylococcus aureus* in random samples of a normal population. J Hyg (Lond). 1967; 65:567–573. [PubMed: 5235259]

Novick R. Autoinduction and signal transduction in the regulation of staphylococcal virulence. Mol Microbiol. 2003; 48:1429–1449. [PubMed: 12791129]

Novick R, Jiang D. The staphylococcal *saeRS* system coordinates environmental signals with *agr* quorum sensing. Microbiology. 2003; 149:2709–2717. [PubMed: 14523104]

Novick RP. Genetic systems in staphylococci. Methods Enzymol. 1991; 204

Olson M, Nygaard T, Ackermann L, Watkins R, Zurek O, Pallister K, Griffith S, Kiedrowski M, Flack C, Kavanaugh J, Kreiswirth B, Horswill A, Voyich J. *Staphylococcus aureus* nuclease is an SaeRS-dependent virulence factor. Infect Immun. 2013; 81:1316–1324. [PubMed: 23381999]

Paulus, H. Biosynthesis of the aspartate family of amino acids. In: Sonenshein, AL.; Hoch, JA.; Losick, R., editors. *Bacillus subtilis* and Other Gram-Positive Bacteria. American Society for Microbiology; Washington, DC: 1993. p. 237-267.

Pohl K, Francois P, Stenz L, Schlink F, Geiger T, Herbert S, Goerke C, Schrenzel J, Wolz C. CodY in *Staphylococcus aureus*: a regulatory link between metabolism and virulence gene expression. J Bacteriol. 2009; 191:2953–2963. [PubMed: 19251851]

Recsei P, Kreiswirth B, O'Reilly M, Schlievert P, Gruss A, Novick R. Regulation of exoprotein gene expression in *Staphylococcus aureus* by *agr*. Mol Gen Genet. 1986; 202:58–61. [PubMed: 3007938]

Rodionov DA, Vitreschak AG, Mironov AA, Gelfand MS. Comparative genomics of the methionine metabolism in Gram-positive bacteria: a variety of regulatory systems. Nucleic Acids Res. 2004; 32:3340–3353. [PubMed: 15215334]

Rogasch K, Ruhmling V, Pane-Farre J, Hoper D, Weinberg C, Fuchs S, Schmudde M, Broker BM, Wolz C, Hecker M, Engelmann S. Influence of the two-component system SaeRS on global gene expression in two different Staphylococcus aureus strains. J Bacteriol. 2006; 188:7742–7758. [PubMed: 17079681]

Roux A, Todd D, Velázquez J, Cech N, Sonenshein A. CodY-mediated regulation of the *Staphylococcus aureus* Agr system integrates nutritional and population density signals. J Bacteriol. 2014; 196:1184–1196. [PubMed: 24391052]

Ruiz de los Mozos I, Vergara-Irigaray M, Segura V, Villanueva M, Bitarte N, Saramago M, Domingues S, Arraiano CM, Fechter P, Romby P, Valle J, Solano C, Lasa I, Toledo-Arana A. Base pairing interaction between 5'- and 3'-UTRs controls icaR mRNA translation in *Staphylococcus aureus*. PLos Genet. 2013; 9:e1004001. [PubMed: 24367275]

Sadykov MR, Mattes TA, Luong TT, Zhu Y, Day SR, Sifri CD, Lee CY, Somerville GA. Tricarboxylic acid cycle-dependent synthesis of *Staphylococcus aureus* Type 5 and 8 capsular polysaccharides. J Bacteriol. 2010; 192:1459–1462. [PubMed: 20061474]

Salgado-Pabón W, Breshears L, Spaulding A, Merriman J, Stach C, Horswill A, Peterson M, Schlievert P. Superantigens are critical for *Staphylococcus aureus* Infective endocarditis, sepsis, and acute kidney injury. MBio. 2013; 4:e00494–00513. [PubMed: 23963178]

Sassi M, Sharma D, Brinsmade S, Felden B, Augagneur Y. Genome Sequence of the Clinical Isolate *Staphylococcus aureus* subsp. *aureus* Strain UAMS-1. Genome Announc. 2015; 3:e01584–01514. [PubMed: 25676774]

Schenk S, Laddaga RA. Improved method for electroporation of Staphylococcus aureus. FEMS Microbiol Lett. 1992; 73:133–138. [PubMed: 1521761]

Schleifer KH, Kandler O. Peptidoglycan types of bacterial cell walls and their taxonomic implications. Bacteriol Rev. 1972; 36:407–477. [PubMed: 4568761]

Schoenfelder SM, Marincola G, Geiger T, Goerke C, Wolz C, Ziebuhr W. Methionine biosynthesis in Staphylococcus aureus is tightly controlled by a hierarchical network involving an initiator tRNA-specific T-box riboswitch. PLoS Pathog. 2013; 9:e1003606. [PubMed: 24068926]

Somerville GA, Proctor RA. At the crossroads of bacterial metabolism and virulence factor synthesis in Staphylococci. Microbiol Mol Biol Rev. 2009; 73:233–248. [PubMed: 19487727]

Tavazoie S, Hughes JD, Campbell MJ, Cho RJ, Church GM. Systematic determination of genetic network architecture. Nat Genet. 1999; 22:281–285. [PubMed: 10391217]

Thomas DY, Jarraud S, Lemercier B, Cozon G, Echasserieau K, Etienne J, Gougeon ML, Lina G, Vandenesch F. Staphylococcal enterotoxin-like toxins U2 and V, two new staphylococcal superantigens arising from recombination within the enterotoxin gene cluster. Infect Immun. 2006; 74:4724–4734. [PubMed: 16861660]

Tsang LH, Cassat JE, Shaw LN, Beenken KE, Smeltzer MS. Factors contributing to the biofilm-deficient phenotype of S*taphylococcus aureus sarA* mutants. PLoS One. 2008; 3:e3361. [PubMed: 18846215]

Valentino M, Foulston L, Sadaka A, Kos V, Villet R, Santa Maria JJ, Lazinski D, Camilli A, Walker S, Hooper D, Gilmore M. Genes contributing to *Staphylococcus aureus* fitness in abscess- and infection-related ecologies. MBio. 2014; 5:e01729–01714. [PubMed: 25182329]

Vallejo AN, Pogulis RJ, Pease LR. PCR mutagenesis by overlap extension and gene SOE. CSH Protoc. 2008 2008:pdb.prot4861.

Vandenesch F, Naimi T, Enright M, Lina G, Nimmo G, Heffernan H, Liassine N, Bes M, Greenland T, Reverdy M, Etienne J. Community-acquired methicillin-resistant *Staphylococcus aureus* carrying Panton-Valentine leukocidin genes: worldwide emergence. Emerg Infect Dis. 2003; 9:978–984. [PubMed: 12967497]

Villapakkam AC, Handke LD, Belitsky BR, Levdikov VM, Wilkinson AJ, Sonenshein AL. Genetic and biochemical analysis of the interaction of *Bacillus subtilis* CodY with branched-chain amino acids. J Bacteriol. 2009; 191:6865–6876. [PubMed: 19749041]

Voyich J, Braughton K, Sturdevant D, Whitney A, Saïd-Salim B, Porcella S, Long R, Dorward D, Gardner D, Kreiswirth B, Musser J, DeLeo F. Insights into mechanisms used by *Staphylococcus aureus* to avoid destruction by human neutrophils. J Immunol. 2005; 175:3907–3919. [PubMed: 16148137]

Weinberg E. Nutritional immunity. Host's attempt to withold iron from microbial invaders. JAMA. 1975; 231:39–41. [PubMed: 1243565]

Wu S, de Lencastre H, Tomasz A. Sigma-B, a putative operon encoding alternate sigma factor of *Staphylococcus aureus* RNA polymerase: molecular cloning and DNA sequencing. J Bacteriol. 1996; 178:6036–6042. [PubMed: 8830703]

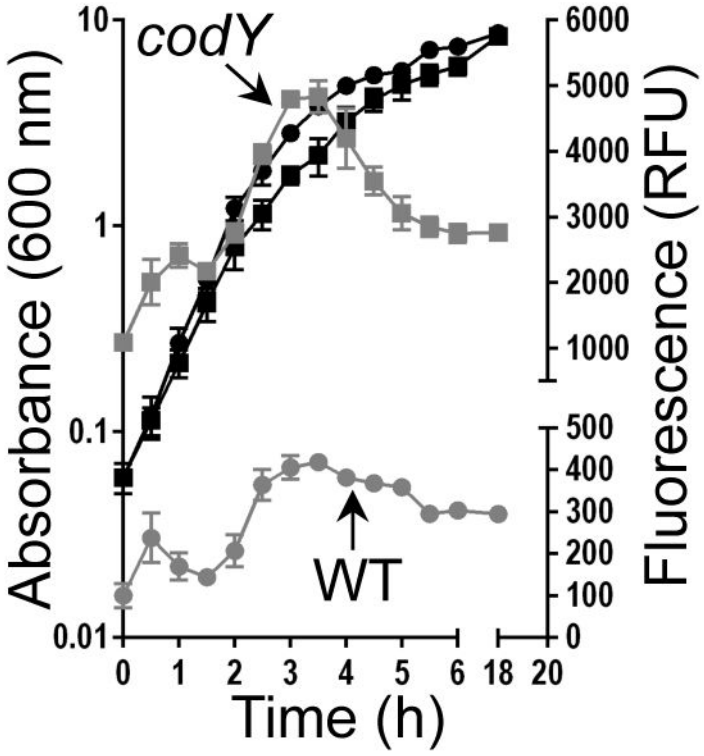

Fig. 1. Post-exponential nutrient limitation does not relieve strong CodY-mediated *nuc* repression

S. aureus UAMS-1 and the *codY* null mutant carrying the *nuc-gfp* reporter were grown in TSB medium (black curves). At the indicated times, samples were withdrawn, washed and resuspended in PBS buffer and GFP fluorescence was measured, normalizing fluorescence to cell growth (Relative Fluorescence Units [RFUs]; grey curves). The data are presented as mean ± SEM from two independent experiments. Where error bars appear absent, they are obscured by the curve symbol. UAMS-1, circles; *codY* null mutant, squares.

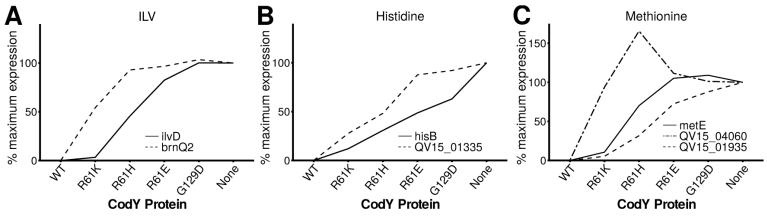

Fig. 2. *S. aureus* prioritizes amino acid uptake in response to reductions in CodY activity

All data here and in subsequent figures are presented as the means of at least two independent experiments. RNA-Seq data are shown; % maximal expression relative to the *codY* null mutant (SRB372, None) is plotted across strains producing varying amounts of CodY regulatory activity: $CodY^{WT}$, SRB337; $CodY^{R61K}$, SRB506; $CodY^{R61H}$, SRB623; $CodY^{R61E}$, SRB577; $CodY^{G129D}$, SRB493. In each panel, genes for nutrient transport are more sensitive to changes in CodY activity and reach 100% prior to genes for nutrient biosynthesis. **A.** CodY-repressed genes coding for the uptake (*brnQ2,* QV15_01265) and synthesis (*ilvD*) of ILV. **B.** CodY-repressed genes coding for the uptake (proposed histidine transporter, QV15_01335) and synthesis (*hisB*) of histidine. **C.** CodY-repressed genes coding for the uptake (*metNIQ1* [QV15_01935-01945], *metNIQ2* [QV15_04055-04065]) and synthesis (*metE*) of methionine.

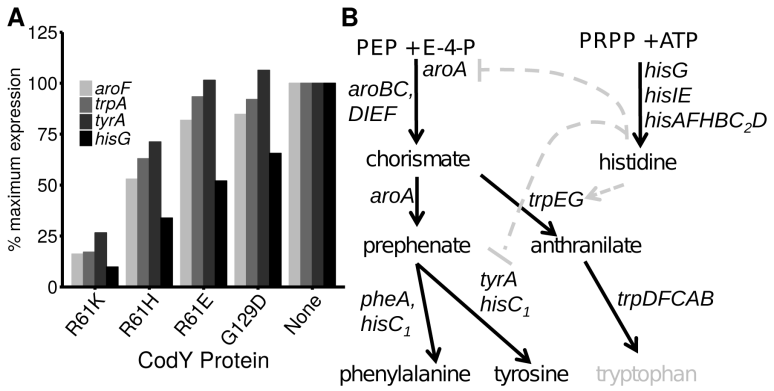

Fig. 3. *S. aureus* represses aromatic amino acid synthesis less stringently than histidine biosynthesis

A. Representative CodY-repressed genes coding for the synthesis of aromatic amino acids and histidine are shown; RNA-Seq data in CodY variant strains are presented as a percentage of the value obtained in the *codY* mutant strain (SRB372, none), set to 100% expression. R61K, SRB506; R61H, SRB623; R61E, SRB577; G129D, SRB493. Genes for aromatic amino acid biosynthesis include *aroF* (chorismate synthase), *trpA* (tryptophan synthase), and *tyrA* (prephenate dehydrogenase). *hisG* encodes ATP phosphoribosyltransferase (catalytic subunit) for histidine biosynthesis. WT, SRB337 was set at 0% and is not shown. **B.** Phenylalanine and tyrosine are derived from the common intermediate prephenate. UAMS-1 is likely a tryptophan auxotroph (grey) due to a frameshift in *trpD*. Histidine is synthesized from phosphoribosyl pyrophosphate (PRPP) and ATP and, at least in *B. subtilis,* influences aromatic amino acid synthesis transcriptionally (*aroA* and *tyrA*) and allosterically (TrpEG), and is indicated by the grey dashed arrows. Arrows, positive effect; blunt arrow, negative effect.

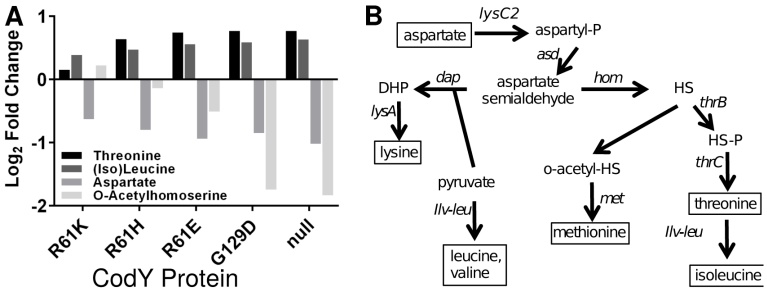

Fig. 4. Metabolite profiling reveals increases in steady state pools of amino acids and biosynthetic intermediates as cognate biosynthetic genes are de-repressed

A. *S. aureus* strains were cultivated exponentially in TSB medium and sampled at OD_{600}~0.5-0.6. Changes in relative intracellular abundance of selected amino acids and biosynthetic intermediates are shown and plotted on a $\log_2$ scale relative to UAMS-1. Mean intracellular metabolite abundances are >1.5-fold altered in the *codY* null mutant relative to UAMS-1 as judged by a Mann-Whitney U test ($p < 0.05$) and across all six strains as judged by Cuzick's test for trend ($p < 0.01$) (Cuzick, 1985). Complete data and statistical analysis can be found in **Dataset S4**. **B.** Lysine, methionine and threonine are derived from aspartate and are collectively known as the aspartate family of amino acids. Pyruvate serves as a precursor for both lysine and ILV synthesis. The pathway bifurcates at aspartate semialdehyde. Differential expression in the *codY* null mutant suggests increased flux through this pathway. *o*-acetyl-HS, *o*-acetyl homoserine; HS, homoserine; HS-P, homoserine-phosphate.

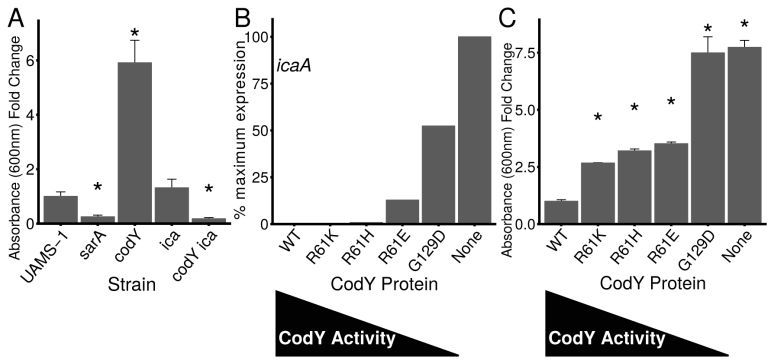

Fig. 5. CodY suppresses PIA-dependent biofilm formation

Strains were grown exponentially for several generations prior to analysis. **A.** Static biofilm development in UAMS-1 strains was measured 24 h following inoculation to tissue culture-treated microtiter plates. Adherent cells were detected by measuring crystal violet retained as absorbance at 600 nm. Data are relative to UAMS-1 (fold change=1). UAMS1, SRB337; UAMS-929, *sarA::kan* (negative control, known to be defective in static biofilm formation); *codY::erm*, SRB372; Δ*ica::tet*, AR11; *codY::erm* Δ*ica::tet*, AR12. Asterisks denote statistically significant comparisons to the *codY* null mutant ($p < 0.05$) using the Games-Howell test (Games *et al.*, 1979). **B.** *icaA* expression data (representative of *ica* locus expression) were extracted from the RNA-Seq data. Values in CodY variant strains are presented as a percentage of the value obtained in the *codY* mutant strain, set to 100% expression. **C.** Static biofilm development in tissue culture-treated microtiter plates indicates that threshold CodY activities promote stepwise increases in static biofilm formation. Adherent cells were detected after 24 h by measuring crystal violet retained as increase in absorbance at 600 nm. Data are relative to UAMS-1 (fold change =1). Asterisks denote statistically significant comparisons to the *codY* null mutant ($p < 0.05$) using the Games-Howell test (Games *et al.*, 1979).

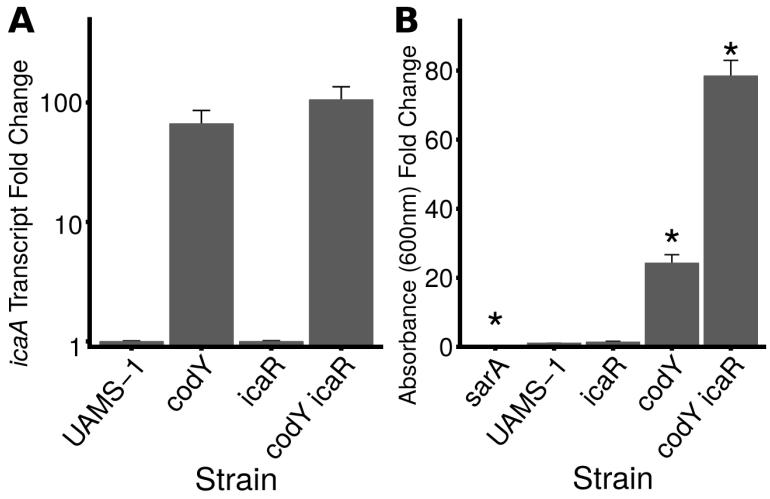

Fig 6. CodY is epistatic to IcaR

Strains were grown exponentially for several generations prior to analysis. In both panels, data are relative to UAMS-1 (fold change=1). **A.** qRT-PCR measurement of *icaA* transcript abundance during exponential growth suggests that CodY overrides loss of IcaR-mediated repression of the *ica* locus. The transcript abundance of *icaA* in UAMS-1 and in the *icaR* null mutant was below the limit of detection (0.08 copies of *icaA* relative to *rpoC*). **B.** Static biofilm development of derivatives of UAMS-1 was measured 24 h following inoculation to tissue culture-treated microtiter plates. Adherent cells were detected by measuring crystal violet retained as absorbance at 600 nm. Asterisks denote statistically significant comparisons to the *codY* null mutant ($p < 0.05$) using the Games-Howell test (Games *et al.*, 1979). UAMS-1, SRB337; *icaR::*φNΣ, SRB813; *codY::* φNΣ[*erm::tet*(M)], SRB814; *icaR::*φNΣ *codY::*φNΣ[*erm::tet*(M)], SRB817. *sarA::kan* (UAMS-929) was used as a negative control because of its known role in static biofilm development.

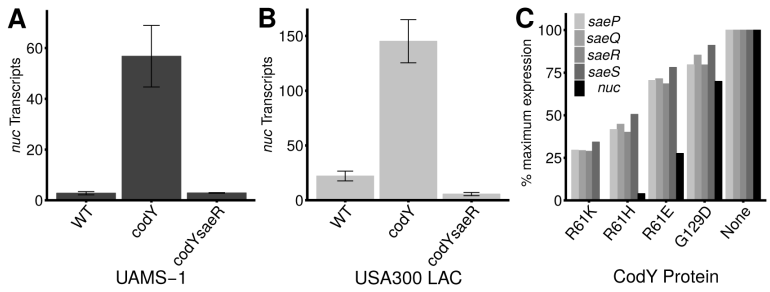

Fig. 7. CodY regulates thermonuclease expression via the Sae TCS

Overexpression of *nuc* in a *codY* mutant requires *saeR.* Strains were grown exponentially and *nuc* transcript abundance measured using qRT-PCR. Data are presented as the mean ± standard error of at least two independent experiments. **A.** UAMS-1: WT, SRB337; *codY::erm*, SRB372; *codY::erm saeR::*φΝΣ[*erm::tet*(M)], SRB759. **B.** USA300 LAC: WT, SRB687; *codY,* SRB746; *codY saeR::*φΝΣ[*erm::tet*(M)], SRB761. **C.** Loss of CodY-mediated repression at *saePQRS* leads to subsequent loss of *nuc* repression. CodY-repressed gene targets coding for the Sae TCS (*saePQRS*) and thermonuclease (*nuc*) are shown. Values in CodY variant strains are presented as a percentage of the value obtained in the *codY* mutant strain, set to 100% expression.

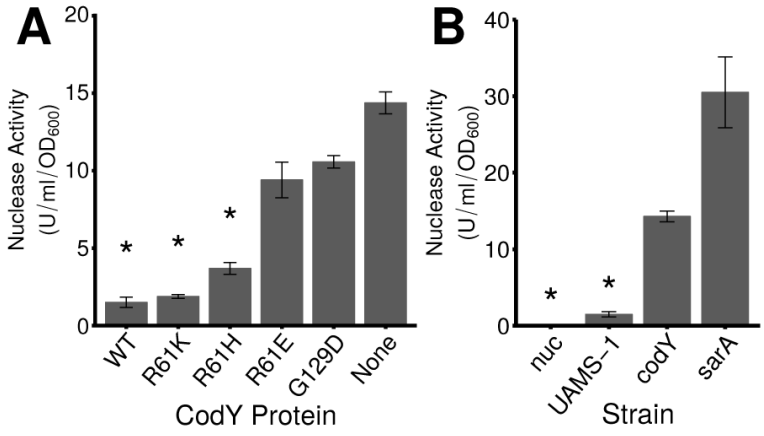

Fig. 8. CodY controls the secretion of thermonuclease in exponentially growing cells

A. Secreted thermonuclease activity in exponentially growing UAMS-1 cell culture supernatants was quantified using a FRET-based assay in strains producing varying amounts of residual CodY activity as described in *Experimental Procedures*. UAMS-1 (WT), SRB337; *codY* null mutant (None), SRB372; and the CodY variants R61K (SRB506), R61H (SRB508), R61E (SRB577) and G129D (SRB493). **B.** Secreted nuclease activity in a CodY-deficient strain relative to a SarA-deficient strain during exponential growth in TSB. *nuc*, UAMS-1471; UAMS-1, SRB337; *codY*, SRB372; *sarA,* UAMS-929. SarA has been shown previously to suppress Nuc enzyme levels (Kiedrowski et al., 2011) and was used as a positive control. Asterisks (*) denote statistical significance by Games-Howell pairwise test ($p < 0.05$) when compared to the *codY* null mutant. The data are presented as the mean ± the standard error of at least 2 independent experiments.

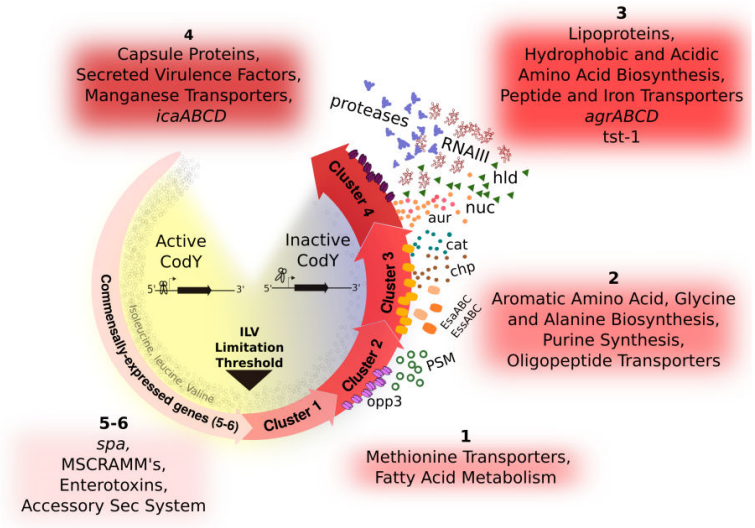

Fig. 9. Working model for how a spectrum of CodY activities generates a developmental program based on the availability of ILV and GTP

During periods of nutrient sufficiency, CodY is active and promotes colonization or persistence on or within the host. Under conditions of increasing nutrient depletion, CodY turns off these commensal lifestyle genes and sequentially turns on (by loss of repression) genes required for transporting preformed compounds, de novo amino acid synthesis, and virulence factors to subvert host defenses and damage host cells and tissues. Salvaging ILV and purines from the host adjusts CodY-dependent gene expression appropriate for that microenvironment.

Table 1

Transcript abundance of CodY-repressed targets during ILV titration.

			ilvD		*hld*	
Relevant genotype	**[ILV] (μM)**	**doubling time (min)**	**Transcript[1]**	**% expression[2]**	**Transcript**	**% expression**
WT[3]	1,500	56 (3)	0.03 (0.001)	0	8.8 (1.9)	0
	150	53 (5)	0.05 (0.006)	0.5	11.5 (3.4)	0.5
	15	120 (21)	7.60 (1.40)	173	81.9 (3.9)	14
	1.5	99 (9)	5.20 (0.90)	118	60.1 (7.4)	10
codY	1,500	66 (2)	4.40 (0.37)	100	518.9 (159.1)	100

[1]Transcript abundance normalized to *polC* abundance during growth in CDM containing the indicated concentration of ILV. Data are presented as the means (SEM) of at least two independent experiments.

[2]% expression calculated using the equation: $((WT_{[ILV]}\text{-}WT_{1500})/(codY_{1500}/WT_{1500})) \times 100$.

[3]UAMS-1

Table 2

RNA-Seq Data Validation

		qRT-PCR		RNA-Seq	
		transcript abundance	% expression[1]	RPKMO value	% expression[1]
	WT	1 (0)[2]	0	4 (0)	0
	R61K	6 (1)	2	51 (6)	3
ilvD	R61H	68 (7)	28	652 (77)	46
	R61E	132 (7)	56	1176 (40)	82
	G129D	216 (35)	91	1429 (15)	100
	Δ *codY*	236 (32)	100	1427 (5)	100
	WT	18 (1)	0	108 (13)	0
	R61K	59 (13)	3	402 (129)	5
hld	R61H	81 (6)	5	554 (104)	8
	R61E	293 (4)	20	1912 (286)	31
	G129D	894 (321)	65	5479 (2562)	93
	Δ *codY*	1364 (44)	100	5887 (1438)	100
	WT	6 (1)	0	107 (1)	0
	R61K	8 (2)	1	115 (9)	0
nuc	R61H	16 (1)	3	196 (3)	4
	R61E	54 (2)	17	722 (2)	28
	G129D	137 (5)	45	1666 (234)	70
	Δ *codY*	297 (40)	100	2337 (116)	100
	WT	7 (0)	0	84 (0)	0
	R61K	43 (2)	33	469 (6)	54
brnQ2	R61H	60 (7)	48	743 (24)	93
	R61E	80 (3)	66	770 (20)	97
	G129D	95 (2)	79	818 (21)	103
	Δ *codY*	117 (25)	100	794 (22)	100
	WT	22 (7)	100	271 (45)	100
	R61K	30 (5)	141	318 (26)	119
fnbA	R61H	22 (2)	101	242 (24)	88
	R61E	6 (1)	15	75 (6)	20
	G129D	4 (1)	8	42 (3)	7
	Δ *codY*	3 (1)	0	25 (0)	0

[1] Set to 100% in the strain where the expression is maximal (UAMS-1 [WT] for stimulated genes, Δ*codY* for repressed genes using the equation ((mutant-WT)/(*codY*-WT)) × 100. Intermediate values are calculated on this scale.

[2] Data are presented as the mean and (standard error) of ≥ two biological replicates.

Table 3

S. aureus strains used.

Strain	Description or genotype	Source or reference[a]
AR2	Newman Δ*ica::tet*	GB Pier via AL Sonenshein (Kropec *et al.*, 2005)
AR11	SRB337 Δ*ica::tet*	
AR12	SRB337 Δ*ica::tet* Δ*codY::erm*	
NE1132	JE2 *icaR::*ϕN∑	(Fey *et al.*, 2013)
NE1555	JE2 *codY::*ϕN∑	(Fey *et al.*, 2013)
NE1622	JE2 *saeR::*ϕN∑	(Fey *et al.*, 2013)
RN4220	Restriction-deficient, highly transformable	(Kreiswirth *et al.*, 1983)
MS-1	Δ*codY::erm*	(Majerczyk *et al.*, 2008)
SRB337	USA200 MSSA UAMS-1	(Gillaspy *et al.*, 1995b)
SRB372	SRB337 Δ*codY::erm*	
SRB373	SRB337 Δ*sucD2::cat194*	
SRB487	SRB337 Δ*ilvE1 codY489* CodY^{G129D}	
SRB493	SRB337 *codY489* CodY^{G129D}	
SRB506	SRB337 *codY57* CodY^{R61K}	
SRB577	SRB337 *codY66* CodY^{R61E}	
SRB623	SRB337 *codY58* CodY^{R61H}	
SRB687	USA300 CA-MRSA EmS (LAC*)(AH1263)	A.R. Horswill
SRB742	JE2 *saeR::*ϕN∑[*erm::tet*(M)]	
SRB746	SRB687 Δ*codY::erm*	
SRB759	SRB337 Δ*codY::erm saeR::*ϕN∑[*erm::tet*(M)]	
SRB761	SRB687 Δ*codY::erm saeR::*ϕN∑[*erm::tet*(M)]	
SRB769	SRB337/pMRSI-nuc (*nuc-gfp)*	
SRB770	SRB372/pMRS1-nuc (*nuc-gfp)*	
SRB798	JE2 *codY::*ϕN∑ [*erm::tet*(M)]	
SRB813	SRB337*icaR::*ϕN∑	
SRB814	SRB337 *codY::*ϕN∑[*erm::tet(M)*]	
SRB817	SRB337 *icaR::*ϕN∑ *codY::*ϕN∑[*erm::tet(M)*]	
UAMS-929	UAMS-1 *sarA::kan*	(Blevins *et al.*, 2002)
UAMS-1471	UAMS-1 Δ*nuc*	(Tsang *et a1.*, 2008)

[a]Unless otherwise noted, strains were constructed during the course of this study.